

Theory and Phenomenology of **Dynamical Dark Matter**

A General Framework for Dark-Matter Physics



Brooks Thomas
(University of Hawaii)

**Work done in collaboration
with Keith Dienes:**

[arXiv:1106.4546]

[arXiv:1107.0721]

[arXiv:1203.1923]

[arXiv:1204.4183] also with Shufang Su

[arXiv:1208.0336] also with Jason Kumar

[arXiv:1306.2959] also with Jason Kumar

Dark Matter: The Conventional Wisdom

In most dark-matter models, the dark sector consists of one stable dark-matter candidate χ (or a few such particles). Such a dark-matter candidate must therefore...

- account for essentially the entire dark-matter relic abundance observed by WMAP/Planck: $\Omega_\chi : \Omega_{\text{CDM}} \approx 0.23$.
- Respect observational limits on the decays of long lived relics (from BBN, CMB data, the diffuse XRB, etc.) which require that χ to be *extremely* stable:

$$\tau_\chi \gtrsim 10^{26} \text{ s}$$

← (Age of universe: only $\sim 10^{17}$ s)

Consequences

- Such “hyperstability” is the **only** way in which a single DM candidate can satisfy the competing constraints on its abundance and lifetime.
- The resulting theory is essentially “frozen in time”: Ω_{CDM} changes only due to Hubble expansion, etc.

Is hyperstability really the only path to a viable theory of dark matter?



No. There is another.

...and it follows from this fundamental observation:

A given dark-matter component need not be stable if its abundance at the time of its decay is sufficiently small.

Indeed, a sufficiently small abundance ensures that the disruptive effects of the decay of such a particle will be minimal, and that all constraints from BBN, CMB, etc., will continue to be satisfied.

Thus, as we shall see, a natural alternative to hyperstability involves a **balancing of decay widths against abundances**:

- States with larger abundances must have smaller decay widths, but states with smaller abundances can have larger decay widths.
- As long as decay widths are balanced against abundances across the entire dark sector, all phenomenological constraints can be satisfied!

Dynamical Dark Matter

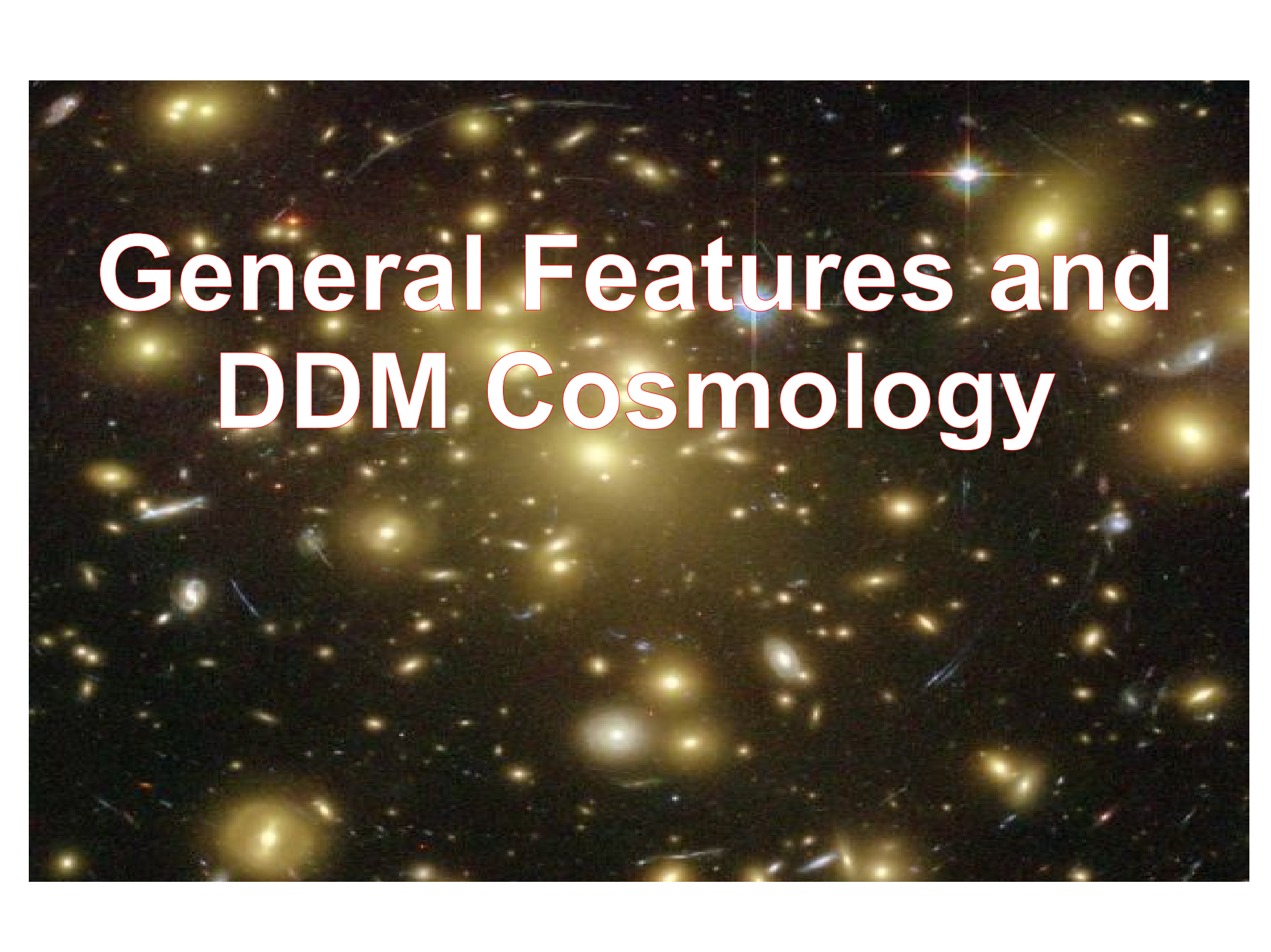
Dynamical Dark Matter (DDM) is a more general framework for dark-matter physics in which these constraints can be satisfied **without** imposing hyperstability.

In particular, in DDM scenarios...

- The dark-matter candidate is an **ensemble** consisting of a vast number of constituent particle species whose collective behavior transcends that of traditional dark-matter candidates.
- Dark-matter stability is not a requirement; rather, the individual abundances of the constituents are **balanced against decay widths** across the ensemble in manner consistent with observational limits.
- Cosmological quantities like the total dark-matter relic abundance, the composition of the dark-matter ensemble, and even the dark-matter equation of state exhibit a **non-trivial time-dependence** beyond that associated with the expansion of the universe.

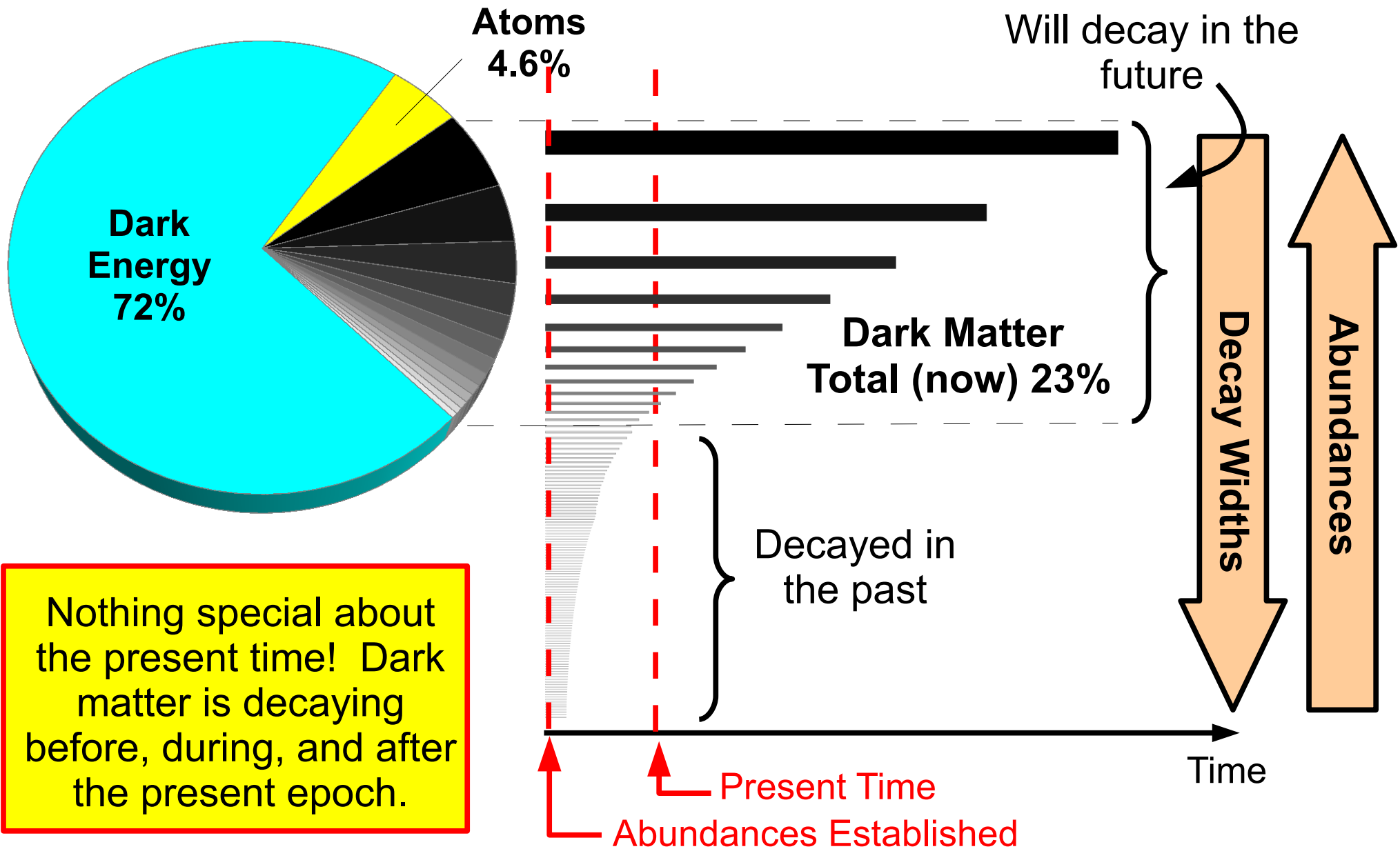
In this talk, I'll be discussing...

- 1 General Features of the DDM framework
- 2 Characterizing the cosmology of DDM models
- 3 An explicit realization of the DDM framework which satisfies all applicable constraints
- 4 Methods for distinguishing DDM ensembles from traditional DM candidates
 - At the LHC
 - At direct detection experiments



General Features and DDM Cosmology

DDM Cosmology: The Big Picture



An example:

For concreteness, consider the case in which the components of the DDM ensemble are scalar fields:

$$\phi_i, i = \{1, \dots, N\} \text{ with } N \gg 1$$

with

$$\begin{array}{l} \text{Masses: } m_i \\ \text{Decay widths: } \Gamma_i \end{array}$$

In a FRW universe, these fields evolve according to

$$\ddot{\phi}_i + (3H + \Gamma_i)\dot{\phi}_i + m_i^2\phi_i = 0$$

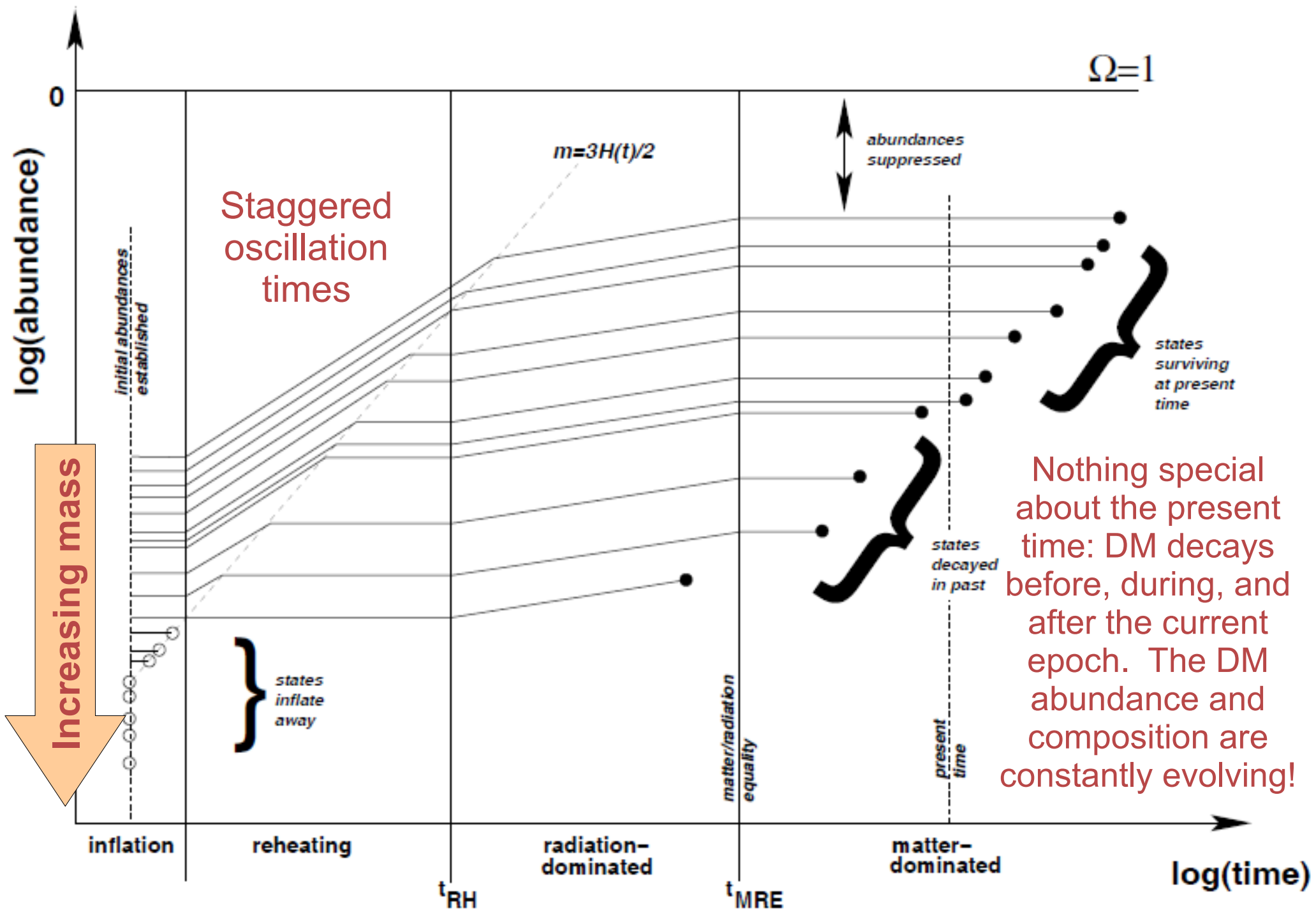
Hubble parameter: $H(t) \sim 1/t$

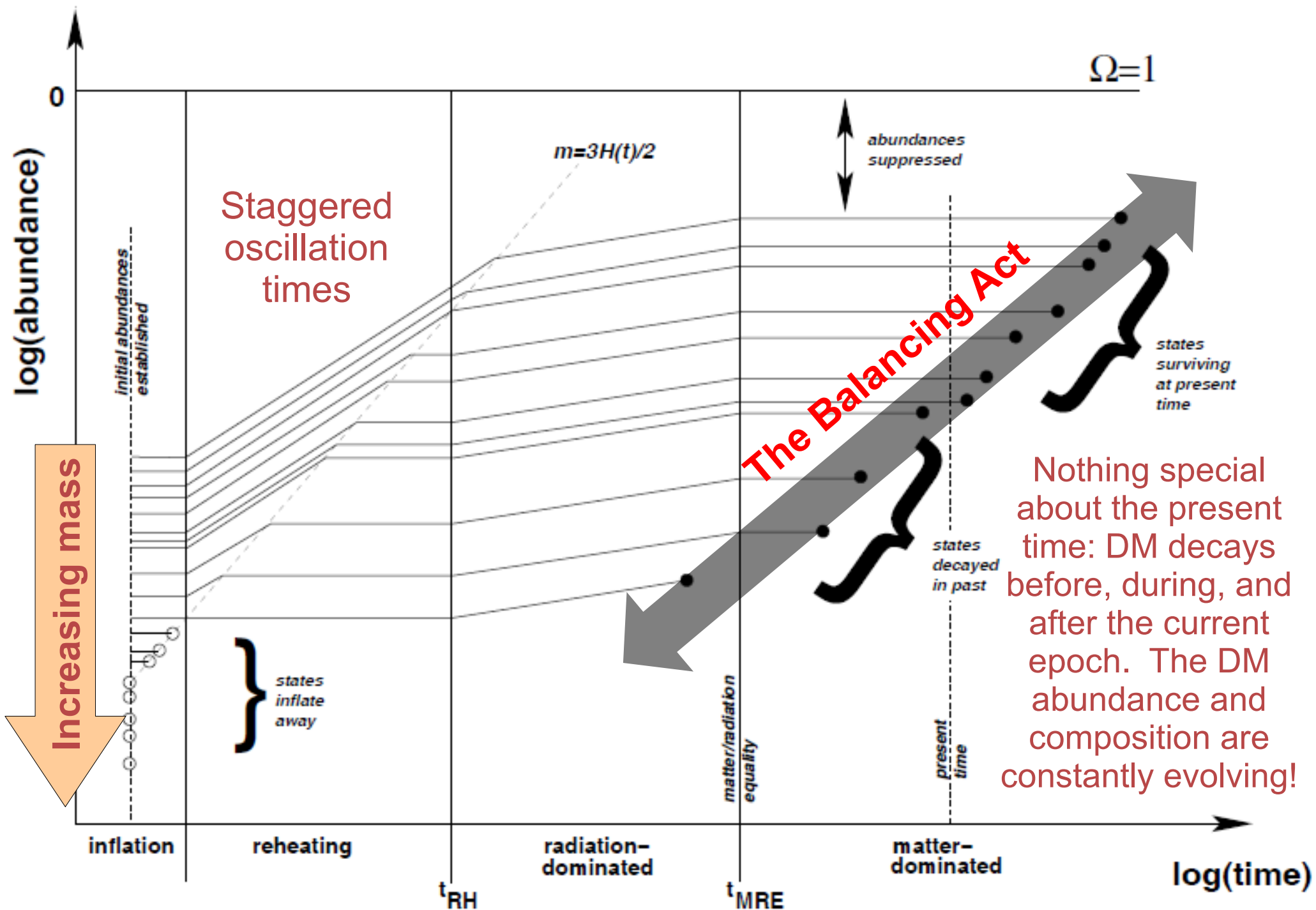
- Each scalar transitions from overdamped to underdamped oscillation at a time t_i , when:

$$3H(t_i) = 2m_i \quad \longrightarrow \quad t_i \sim 1/m_i$$

Heavier states
“turn on” first.

This leads to a dark sector which evolves like...





Nothing special about the present time: DM decays before, during, and after the current epoch. The DM abundance and composition are constantly evolving!

Characterizing DDM Ensembles

- The cosmology of DDM models is principally described in terms of three fundamental (time-dependent) quantities:

1

Total relic abundance:

$$\Omega_{\text{tot}}(t) = \sum_{i=0}^N \Omega_i(t)$$

2

Distribution of that abundance:
(One useful measure)

$$\eta(t) \equiv 1 - \frac{\Omega_0}{\Omega_{\text{tot}}} \quad \text{where} \quad \Omega_0 \equiv \max \{ \Omega_i \}$$

The interpretation:

$$0 \leq \eta \leq 1 \quad \begin{cases} \eta = 0 \\ \eta > 0 \end{cases} \quad \begin{matrix} \longrightarrow & \text{One dominant component} \\ & \text{(standard picture)} \\ & \text{Quantifies departure from traditional DM} \end{matrix}$$

3

Effective equation of state:

$$p = w_{\text{eff}} \rho_{\text{tot}}$$

Not always $w = 0$!

$$w_{\text{eff}}(t) = - \left(\frac{1}{3H} \frac{d\rho_{\text{tot}}}{dt} + 1 \right)$$

Characterizing DDM Ensembles

- Unlike traditional dark-matter candidates, a DDM ensemble has no well-defined mass, decay width, or set of scattering cross-sections.
- The natural parameters which describe such a dark-matter candidate are those which describe **the internal structure of the ensemble** itself and describe how quantities such as the constituent-particle masses, abundances, decay widths, and cross-sections scale with respect to one another across the ensemble as a whole.

For example:

$$\Omega(\Gamma) = A (\Gamma/\Gamma_0)^\alpha$$

$$n_\Gamma(\Gamma) = B(\Gamma/\Gamma_0)^\beta$$

Density of states
per unit width Γ

The properties of the ensemble are naturally expressed in terms of the coefficients A and B and the **scaling exponents** α and β .

e.g., if we take: $\Omega_i(t) \approx \Omega_i \Theta(\tau_i - t)$

$$\sum_i \rightarrow \int n_\tau(\tau) d\tau \quad \text{with} \quad n_\tau = \Gamma^2 n_\Gamma$$

We obtain the
general result:

$$\frac{d\Omega_{\text{tot}}(t)}{dt} \approx - \sum_i \Omega_i \delta(\tau_i - t) \approx -AB\Gamma_0^2 (\Gamma_0 t)^{-\alpha-\beta-2}$$

And from this result follow...

General expressions for our three fundamental quantities:

For $x \equiv \alpha + \beta \neq 1$

For $x \equiv \alpha + \beta = 1$

$\Omega_{\text{tot}}(t)$

$$\Omega_{\text{CDM}} + \frac{AB\Gamma_0}{(1+x)} [(\Gamma_0 t)^{1+x} - \Gamma_0 t_{\text{now}}]^{1+x} \quad \Omega_{\text{CDM}} - AB\Gamma_0 \ln(\Gamma_0 t)$$

$w_{\text{eff}}(t)$

$$\frac{(1+x)w_*}{2w_* + (1+x+2w_*)(t/t_{\text{now}})^{1+x}} \quad \frac{w_*}{1 - 2w_* \ln(t/t_{\text{now}})}$$

where $w_* = \frac{AB\Gamma_0}{2\Omega_{\text{CDM}}(\Gamma_0 t_{\text{now}})^{1+x}}$ where $w_* = \frac{AB\Gamma_0}{2\Omega_{\text{CDM}}}$

$\eta(t)$

$$\frac{2w_* + [\eta_*(1+x) - 2w_*](t/t_{\text{now}})}{2w_{\text{eff}}^* + (1+x+2w_{\text{eff}}^*)(t/t_{\text{now}})^{1+x}} \quad \frac{\eta_* - 2w_* \ln(t/t_{\text{now}})}{1 - 2w_* \ln(t/t_{\text{now}})}$$

Now let's examine an example of how this works for a particular example of a DDM ensemble that arises **naturally** in many extensions of the SM (including string theory)...

An Example: Scalars in Extra Dimensions

- For concreteness, consider a scalar field Φ propagating in a single extra spacetime dimension compactified on a S_1/Z_2 orbifold of radius R . The
- SM fields are restricted to a brane at $x_5=0$.

- The action can in principle include both **bulk-mass** and **brane-mass** terms:

$$S = \int d^4x dy \left[\frac{1}{2} \partial_P \Phi^* \partial^P \Phi - \frac{1}{2} M^2 |\Phi|^2 - \frac{1}{2} \delta(y) m^2 |\Phi|^2 + \mathcal{L}_{\text{int}} \right]$$

KK-mode Mass-Squared Matrix

$$\mathcal{M}_{kl}^2 = \left(\frac{k\ell}{R^2} + M^2 \right) \delta_{kl} + r_k r_\ell m^2$$

Non-renormalizable interactions suppressed by some heavy scale f_ϕ

- Brane mass induces **mixing** among the KK modes: mass eigenstates ϕ_λ are linear combinations of KK-number eigenstates ϕ_k :

$$|\phi_\lambda\rangle = A_\lambda \sum_{k=0}^{\infty} \frac{r_k \tilde{\lambda}^2}{\tilde{\lambda}^2 - k^2 y^2} |\phi_k\rangle$$

$$y = 1/mR$$

Mixing factor: suppresses couplings of light modes to brane states.

$$\text{where } \tilde{\lambda} \equiv \sqrt{\lambda^2 - M^2/m}$$

$$A_\lambda \equiv \frac{\sqrt{2}}{\tilde{\lambda}} \frac{1}{\sqrt{1 + \pi^2/y^2 + \tilde{\lambda}^2}}$$

Balancing from Mixing

The ϕ_λ decay to SM fields on the brane:

Linear combination of ϕ_λ that couples to brane states

Decay widths:

$$\Gamma_\lambda \sim \frac{\lambda^3}{\hat{f}_\phi^2} \langle \phi_\lambda | \phi' \rangle^2 = \frac{\lambda^3}{\hat{f}_\phi^2} (\tilde{\lambda}^2 A_\lambda)^2$$

Relic abundances (from misalignment):

If the 5D field has a shift symmetry $\Phi \rightarrow \Phi + [\text{const.}]$ above the scale at which m is generated, $\phi_{k=0}$ can have a **misaligned vacuum value**:

$$\Omega_\lambda(t_\lambda) \sim \frac{\lambda^2 \theta^2 \hat{f}_\phi^2 |\langle \phi_\lambda | \phi_{k=0} \rangle|^2}{H^2 M_P^2} \left(\frac{t_\lambda}{t} \right)^{\kappa_\lambda} = \frac{\theta^2 \hat{f}_\phi^2}{H^2 M_P^2} \lambda^2 A_\lambda^2 \left(\frac{t_\lambda}{t} \right)^{\kappa_\lambda}$$

Overlap with zero mode

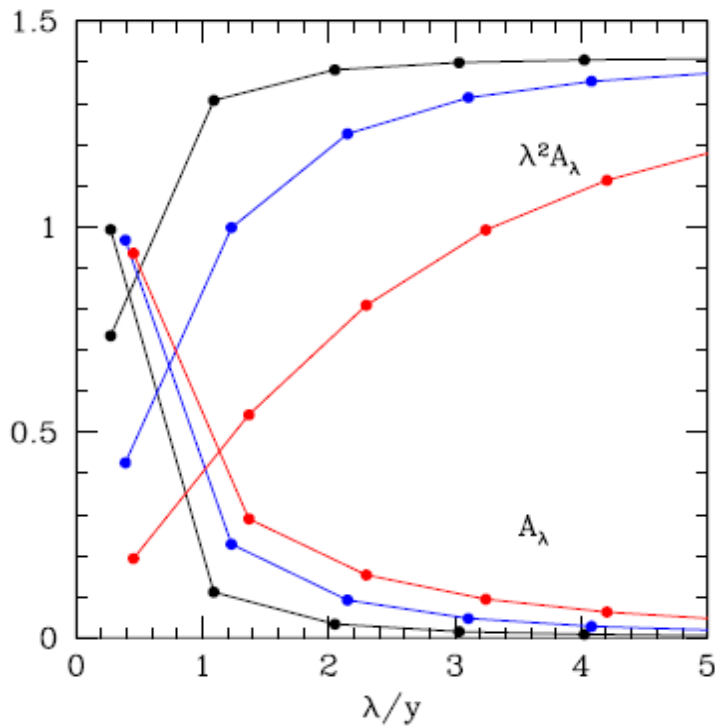
Oscillation-time factor

Staggered: $t_\lambda \sim 1/\lambda$

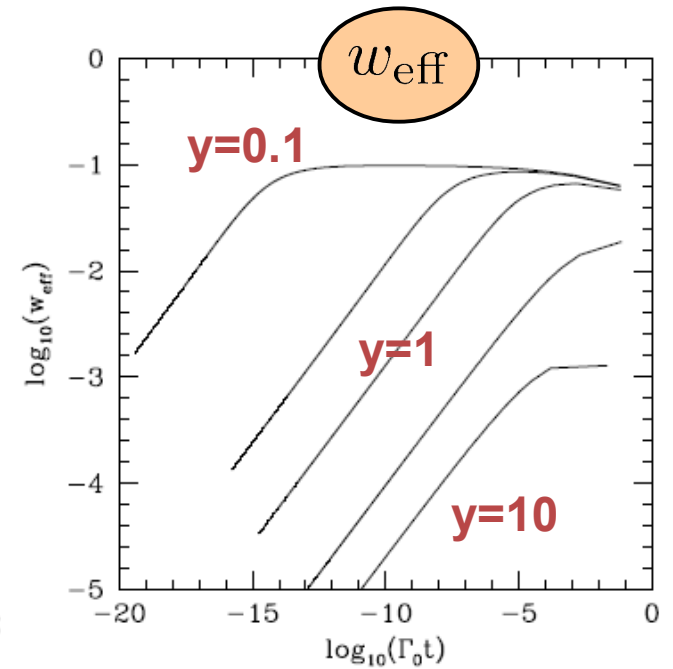
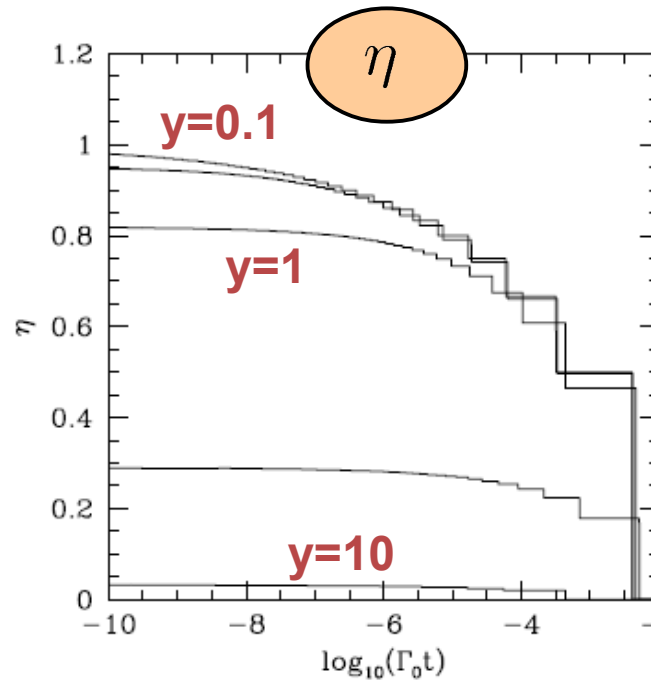
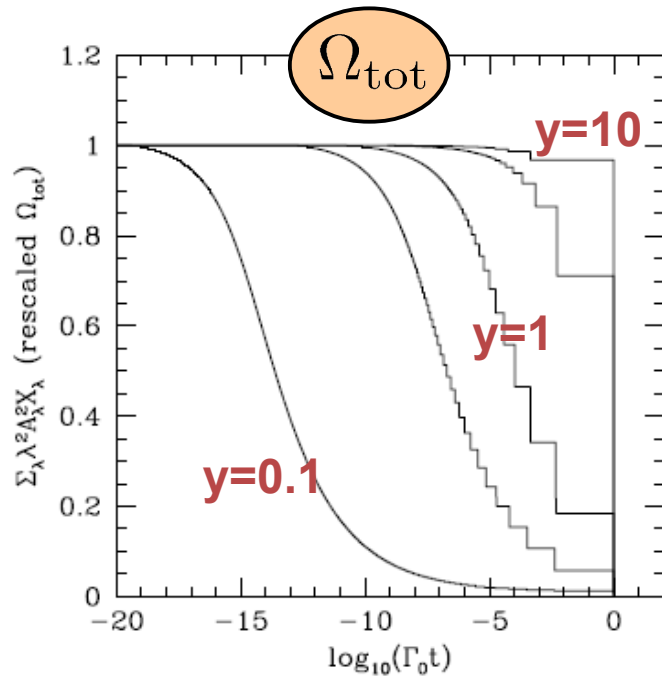
Simultaneous: $t_\lambda \sim \text{const.}$

A natural balance between Ω_λ and Γ_λ !

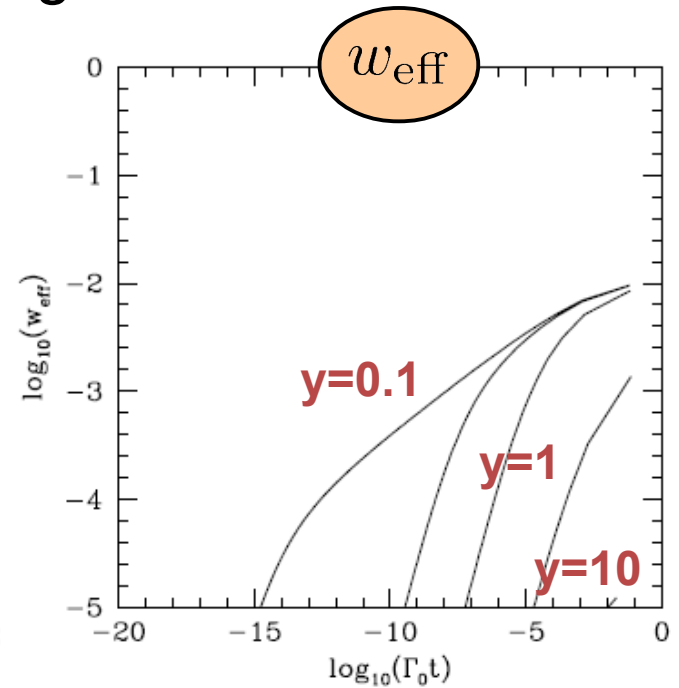
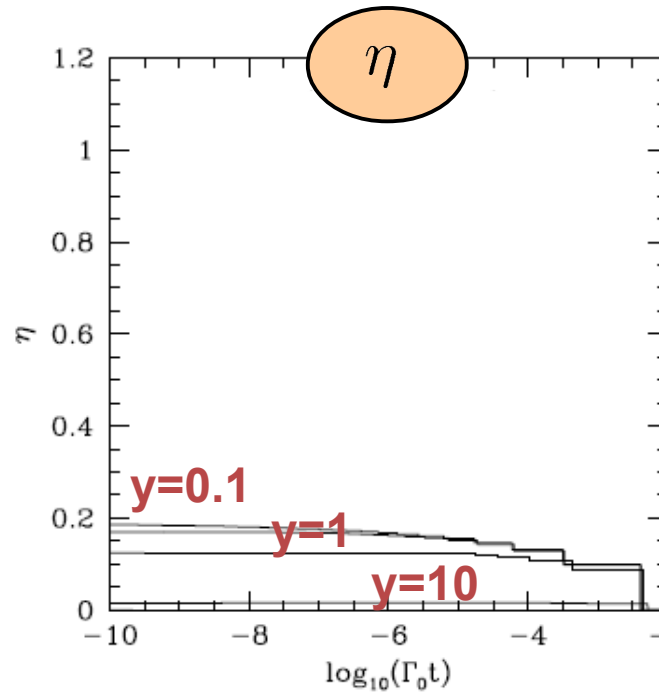
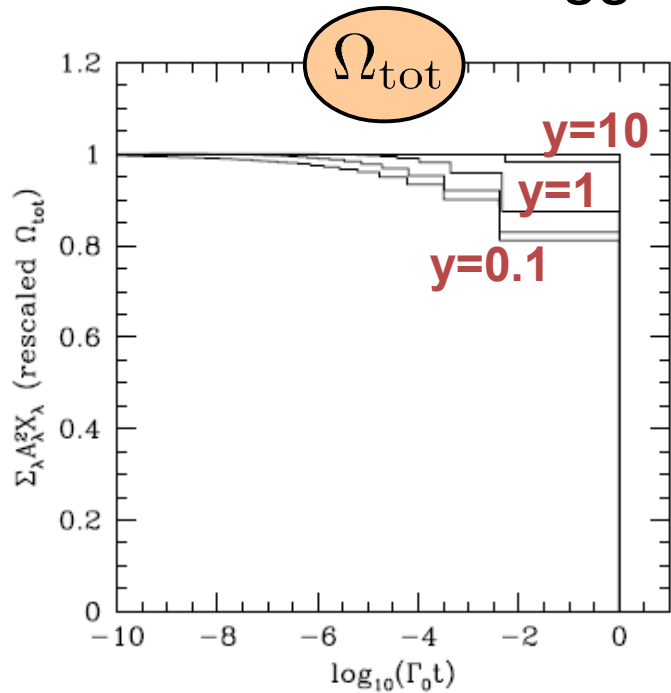
instantaneous :	$\Omega_\lambda \Gamma_\lambda^{2/3} \sim \text{constant}$
staggered (RD era) :	$\Omega_\lambda \Gamma_\lambda^{7/6} \sim \text{constant}$
staggered (reheating/MD era) :	$\Omega_\lambda \Gamma_\lambda^{4/3} \sim \text{constant}$



Simultaneous oscillation:

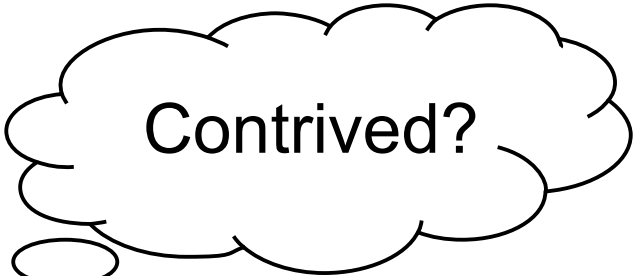


Staggered oscillation times during MD era:

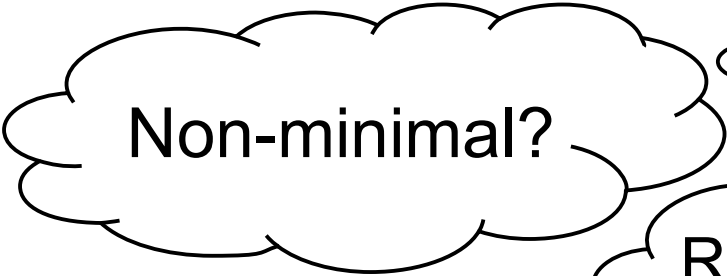


The background of the slide is a vast field of galaxies, likely from the Sloan Digital Sky Survey. The galaxies are of various shapes and sizes, including spirals, ellipticals, and irregulars, scattered across a dark cosmic space. The colors range from bright yellow and orange to deep blues and purples. The text is centered and reads:

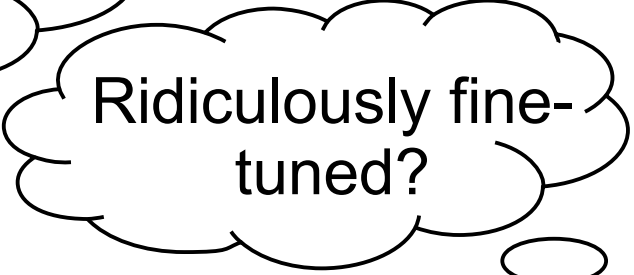
An Explicit DDM Model from Extra Dimensions



Contrived?



Non-minimal?



Ridiculously fine-tuned?

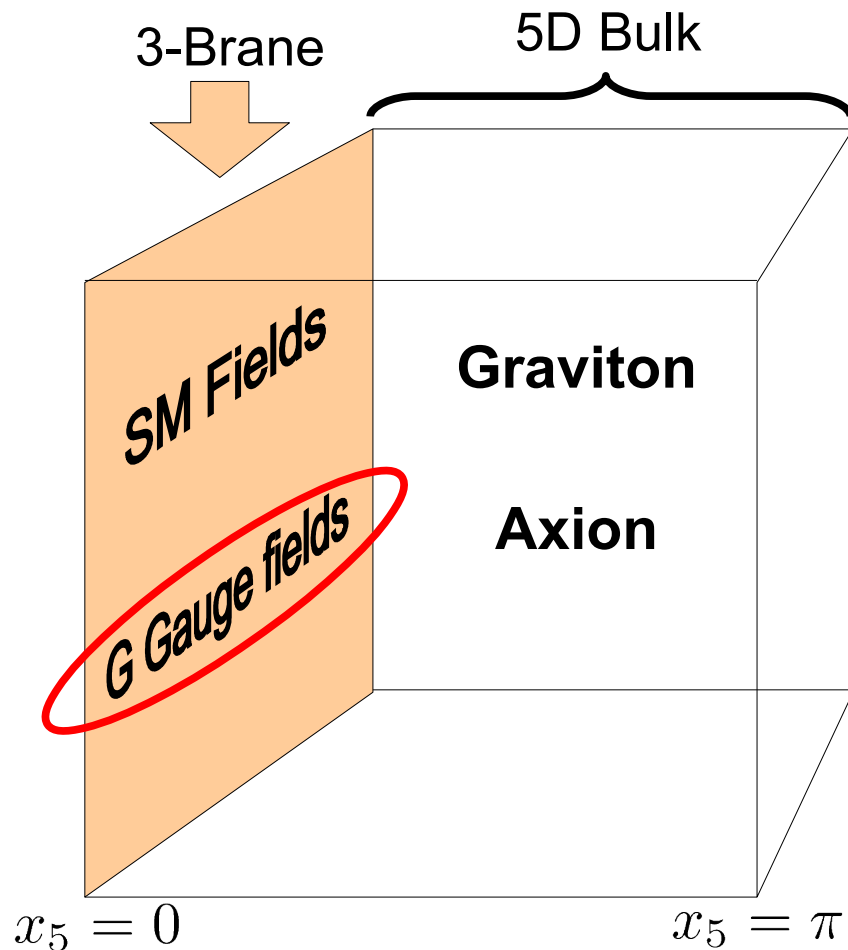
Not at all!

Over the course of this talk, I'll demonstrate how such scenarios arise **naturally** in the context of large extra dimensions.

Moreover, I'll provide an **explicit model** of DDM, in which all applicable constraints are satisfied, and the full ensemble of states contributes significantly toward Ω_{DM} .

This example demonstrates that DDM is a viable framework for addressing the dark-matter question.

(General) Axions in Large Extra Dimensions



- Consider a 5D theory with the extra dimension compactified on S_1/Z_2 with radius $R = 1/M_c$.
- Global $U(1)_X$ symmetry broken at scale f_X by a bulk scalar \rightarrow bulk axion is PNGB.
- SM and an **additional gauge group** G are restricted to the brane. G confines at a scale Λ_G . Instanton effects lead to a **brane-mass** term m_X for the axion.

Axion mass matrix:

$$\begin{pmatrix} m_X^2 & \sqrt{2}m_X^2 & \sqrt{2}m_X^2 & \dots \\ \sqrt{2}m_X^2 & 2m_X^2 + M_c^2 & 2m_X^2 & \dots \\ \sqrt{2}m_X^2 & 2m_X^2 & 2m_X^2 + 4M_c^2 & \dots \\ \vdots & \vdots & \vdots & \ddots \end{pmatrix}$$

When $y \equiv M_c/m_X$ is small, substantial **mixing** occurs:

Mass eigenstates ($\tilde{\lambda} \equiv \lambda/m_X$)

$$a_\lambda = \sum_{n=0}^{\infty} U_{\lambda n} a_n \equiv \sum_{n=0}^{\infty} \left(\frac{r_n \tilde{\lambda}^2}{\tilde{\lambda}^2 - n^2 y^2} \right) A_\lambda a_n$$

“Mixing Factor”

$$A_\lambda = \frac{\sqrt{2}}{\tilde{\lambda}} \left[1 + \tilde{\lambda}^2 + \pi^2/y^2 \right]^{-1/2}$$

The Three Fundamental Questions:

1. “Does the relic abundance come out right?”

$$\Omega_{\text{tot}} \equiv \sum_{\lambda} \Omega_{\lambda} \quad \text{must match} \quad \Omega_{\text{DM}}^{\text{WMAP}} h^2 = 0.1131 \pm 0.0034$$

[Komatsu et al.; '09]

2. “Do a large number of modes contribute to that abundance, or does the lightest one make up essentially all of Ω_{DM} ?”

In other words, is $\eta \sim \mathcal{O}(1)$

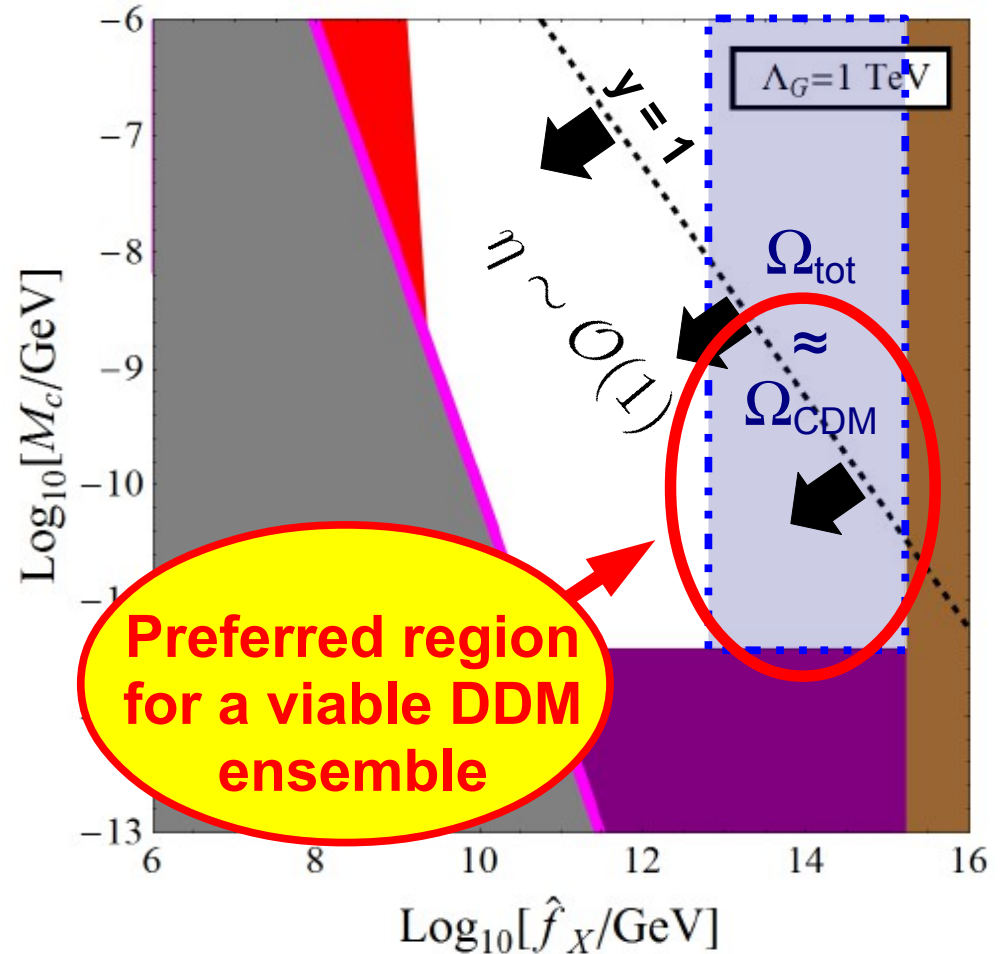
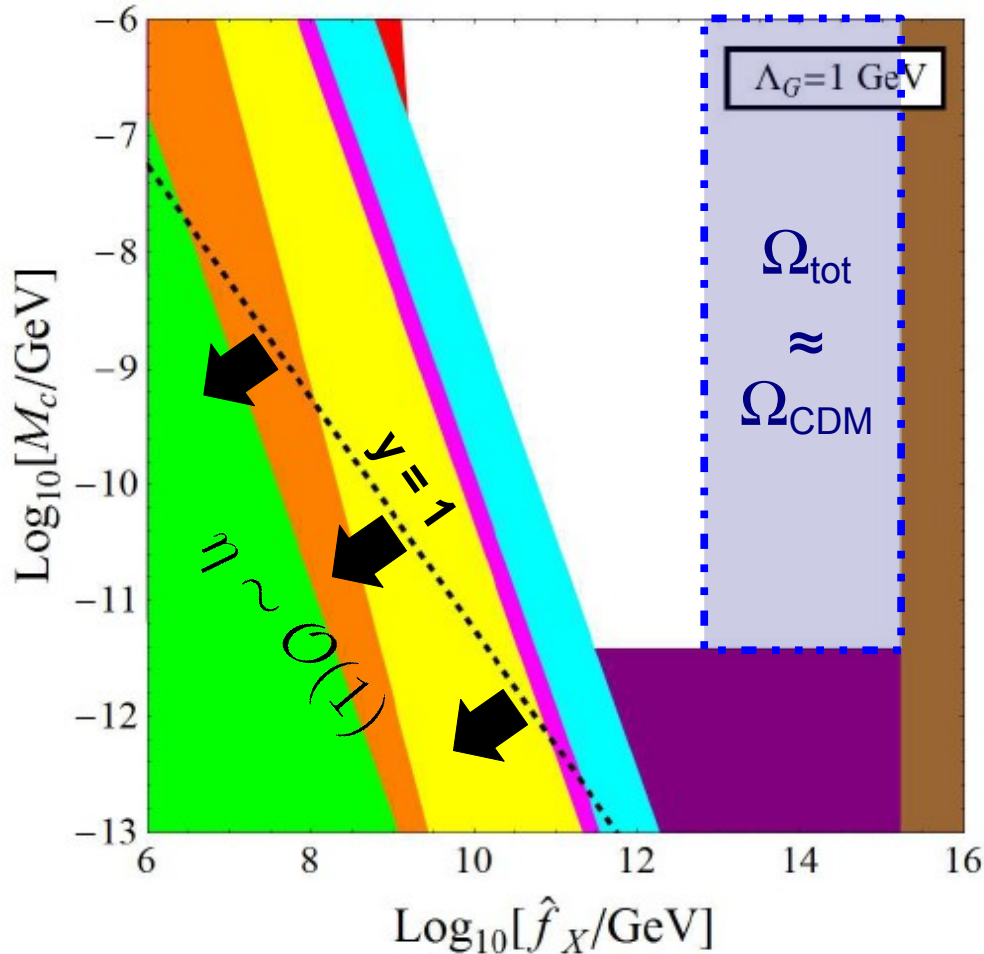
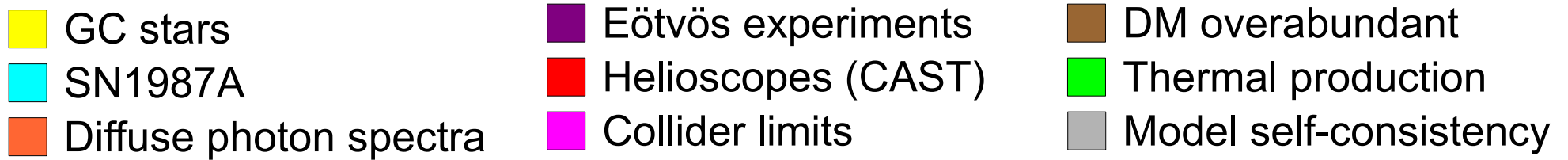
so that the full tower contributes nontrivially to Ω_{DM} ?

3. “Is the model consistent with all of the applicable experimental, astrophysical, and cosmological constraints?”

Thanks to the properties of the mixing factor A_{λ} , the answer to all three questions can indeed (simultaneously) be in the affirmative!

The Result: A Viable DDM Ensemble

- While a great many considerations constrain scenarios involving light bulk axions, they can all be simultaneously satisfied while $\Omega_{\text{tot}} \approx \Omega_{\text{CDM}}$ and $\eta \sim \mathcal{O}(1)$.



Constraints on Axion Models of DDM

- While a great many considerations constrain scenarios involving light bulk axions, they can all be simultaneously satisfied while $\Omega_{\text{tot}} \approx \Omega_{\text{CDM}}$ and $\eta \sim \mathcal{O}(1)$.

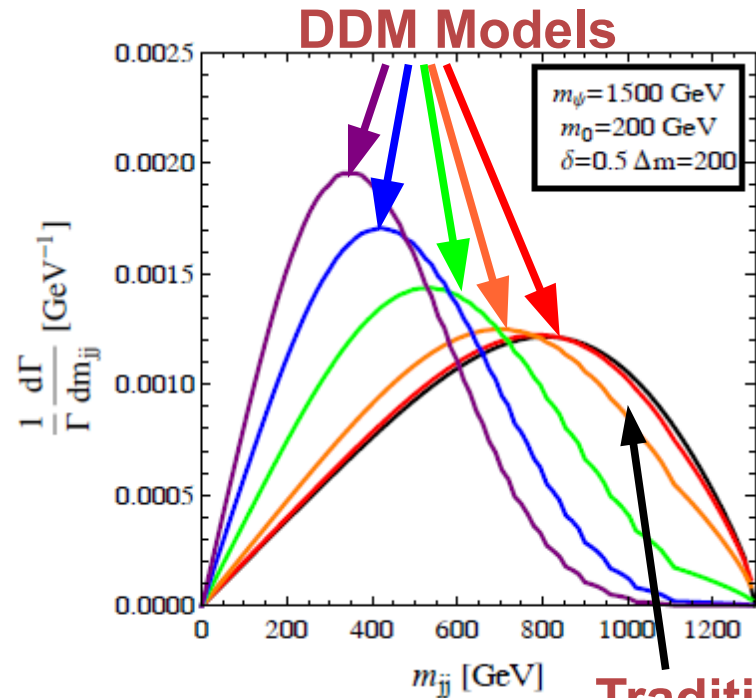
 GC stars	 Eötvös experiments	 DM overabundant
 SN1987A	 Helioscopes (CAST)	 Thermal production
 Diffuse photon spectra	 Collider limits	

...and of course, there's also:

-  Isocurvature perturbations
-  Exotic hadron decays
-  Light-shining-through-walls experiments
-  Microwave-cavity detectors (ADMX)
-  Light-element abundances (BBN)
-  Late entropy production
-  Inflation and primordial gravitational waves

**Within the region of parameter space in which
 $\Omega_{\text{tot}} \sim \Omega_{\text{CDM}}$, these are satisfied too!**

Discovering and Differentiating DDM



At the LHC, ...

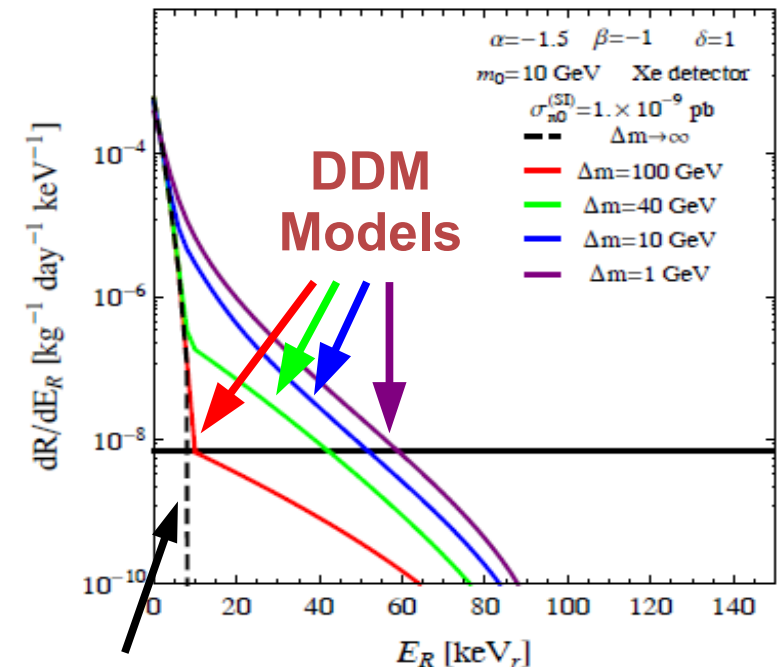
K. R. Dienes, S. Su, BT [arXiv:1204.4183]

- In many DDM models, constituent fields in the DDM ensemble can be produced alongside SM particles by the decays of additional heavy fields.
- Evidence of a DDM ensemble can be ascertained in characteristic features imprinted on the invariant-mass distributions of these SM particles.

at direct-detection experiments, ...

K. R. Dienes, J. Kumar, BT [arXiv:1208.0336]

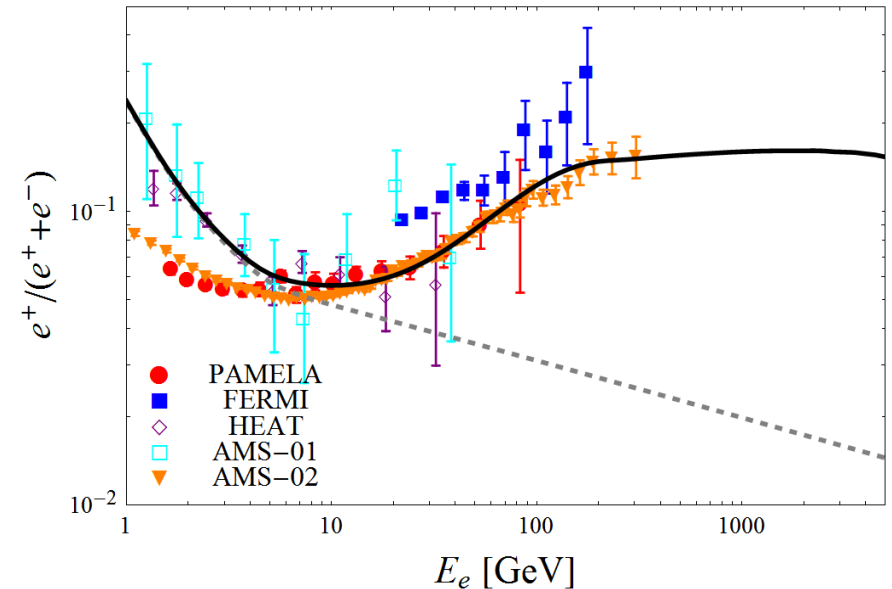
- DDM ensembles can also give rise to distinctive features in recoil-energy spectra.



... and at indirect-detection experiments.

K. R. Dienes, J. Kumar, BT [arXiv:1306.2959]

- DDM ensembles can reproduce the observed positron data from AMS while satisfying constraints from other astrophysical constraints on decaying dark matter.
- Moreover, DDM models of the positron excess give rise to concrete predictions for the behavior of the positron fraction at high energies.



These are just three examples which illustrate that DDM ensembles give rise to **observable effects** which can serve to distinguish them from traditional DM candidates

Let's turn to examine some of the phenomenological possibilities inherent in the DDM framework in greater detail.

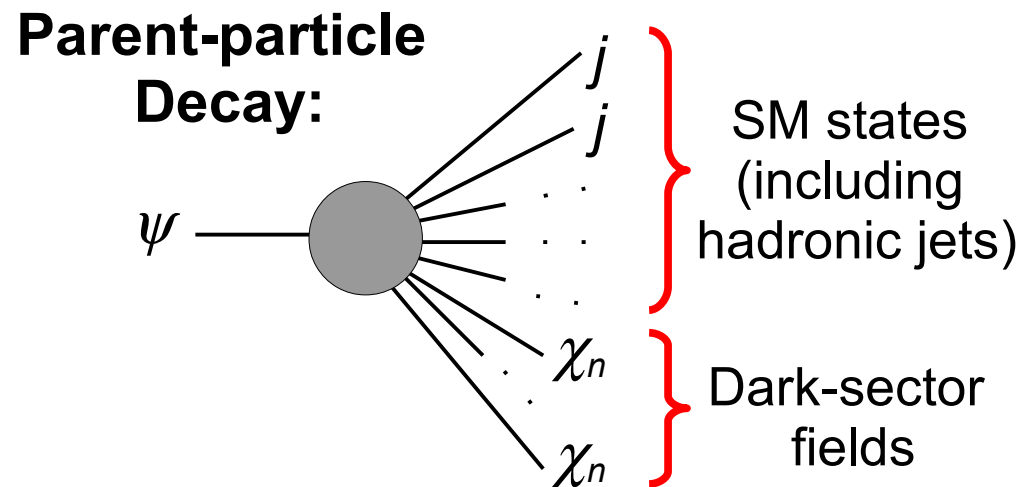
Distinguishing DDM at the LHC



Searching for Signs of DDM at the LHC

- In a wide variety of DM models, dark-sector fields can be produced via the decays of some heavy “**parent particle**” ψ .
- Strongly interacting ψ can be produced copiously at the LHC. $SU(3)_c$ invariance requires that such ψ decay to final states including not only dark-sector fields, but **SM quarks and gluons** as well.
- In such scenarios, the initial signals of dark matter will generically appear at the LHC in channels involving jets and \cancel{E}_T .

Further information about the dark sector or particles can **also** be gleaned from examining the **kinematic distributions** of visible particles produced alongside the DM particles.

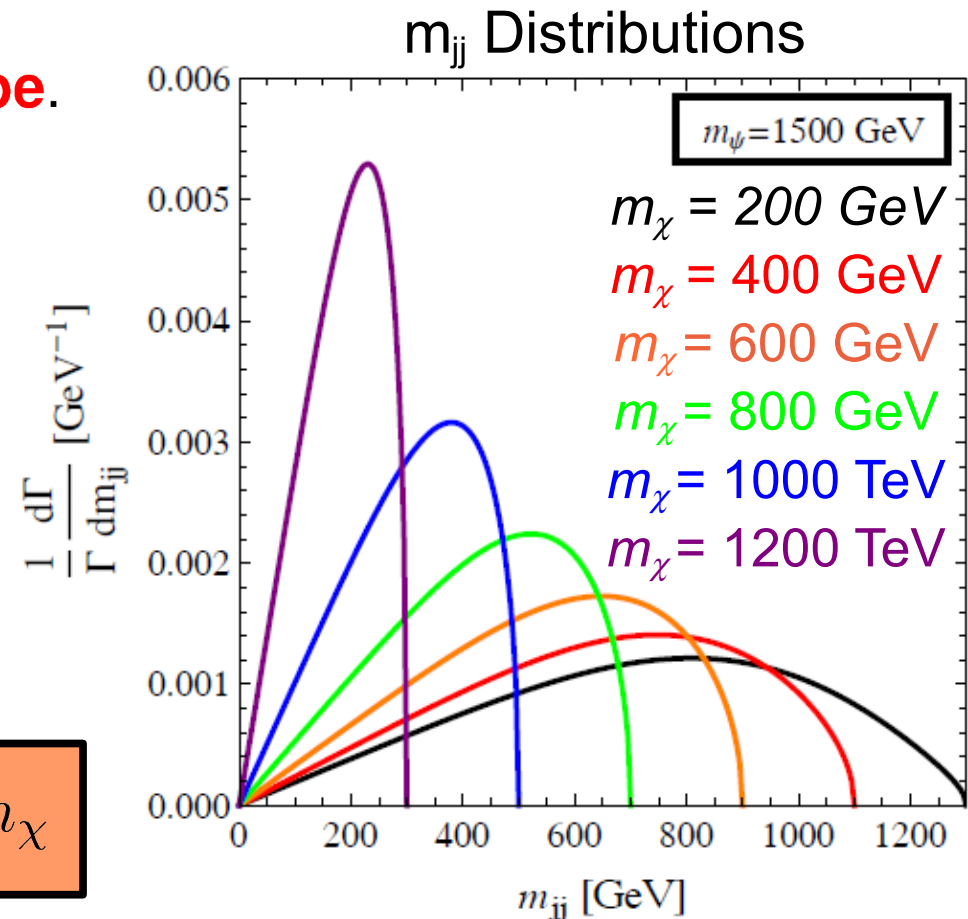


As we shall see, such information can be used to distinguish DDM ensembles from traditional DM candidates on the basis of LHC data.

Traditional DM Candidates

- Let's begin by considering a dark sector which consists of a traditional dark-matter candidate χ — a **stable** particle with a mass m_χ .
- For concreteness, consider the case in which ψ decays primarily via the **three-body** process $\psi \rightarrow jj\chi$ (no on-shell intermediary).
- Invariant-mass distributions for such decays manifest a **characteristic shape**.
- Different coupling structures between ψ , χ , and the SM quark and gluon fields, different representations for ψ , *etc.* have only a small effect on the distribution.
- m_{jj} distributions characterized by the presence of a **mass “edge”** at the kinematic endpoint:

$$m_{jj} \leq m_\psi - m_\chi$$



Parent Particles and DDM Daughters

In general, the constituent particles χ_n in a DDM ensemble and other fields in the theory through some set of effective operators $O_n^{(\alpha)}$:

$$\mathcal{L}_{\text{eff}} = \sum_{\alpha} \sum_{n=0}^N \frac{c_{n\alpha}}{\Lambda^{d_{\alpha}-4}} \mathcal{O}_n^{(\alpha)} + \dots$$

As an example, consider a theory in which the masses and coupling coefficients of the χ_n scale as follows:

m_0 : mass of lightest constituent

$$c_{n\alpha} = c_{0\alpha} \left(\frac{m_n}{m_0} \right)^{\gamma_{\alpha}}$$

$$m_n = m_0 + n^{\delta} \Delta m$$

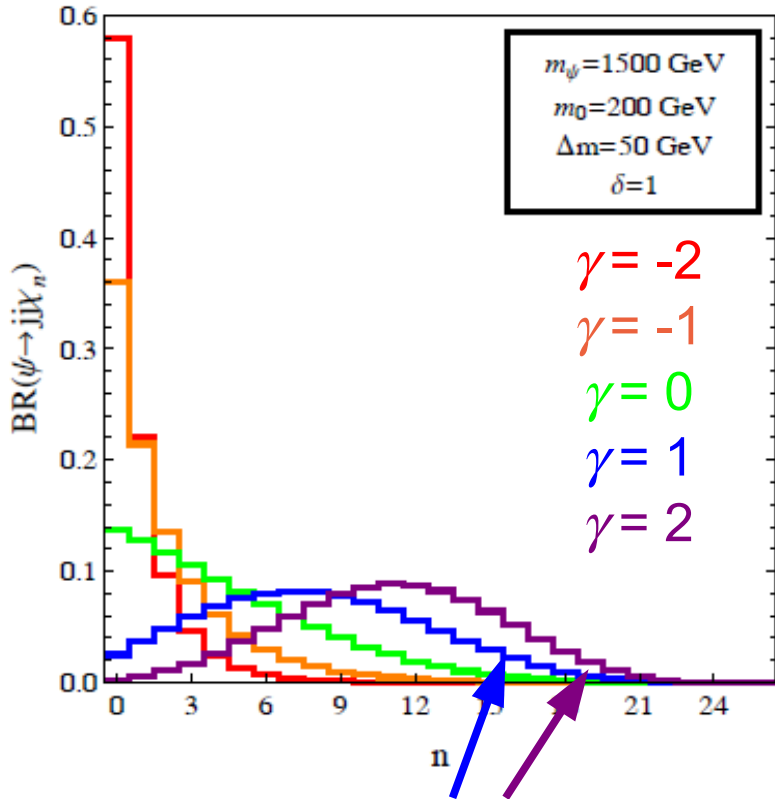
γ_{α} : scaling indices for couplings

Including coupling between ψ and the dark-sector fields χ_n .

δ : scaling index for the density of states

Δm : mass-splitting parameter

Parent-Particle Branching Fractions



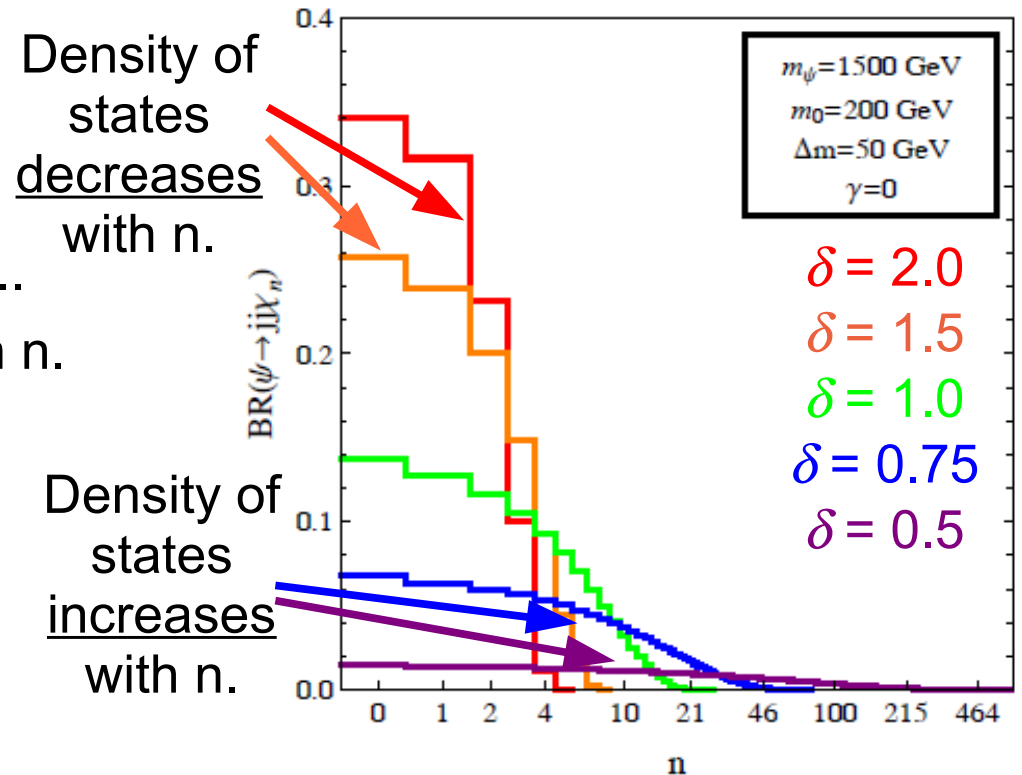
Coupling strength increases with n for $\gamma > 0$...
 ...but phase space always decreases with n .

- **Branching fractions** of ψ to the different χ_n controlled by Δm , δ , and γ .

- Once again, let's consider the simplest non-trivial case in which ψ couples to each of the χ_n via a four-body interaction, e.g.:

$$\mathcal{L}_{\text{eff}} = \sum_n \left[\frac{c_n}{\Lambda^2} (\bar{q}_i t_{ij}^a \psi^a) (\bar{\chi}_n q_j) + \text{h.c.} \right]$$

- Assume parent's total width Γ_ψ dominated by decays of the form $\psi \rightarrow jj\chi_n$.

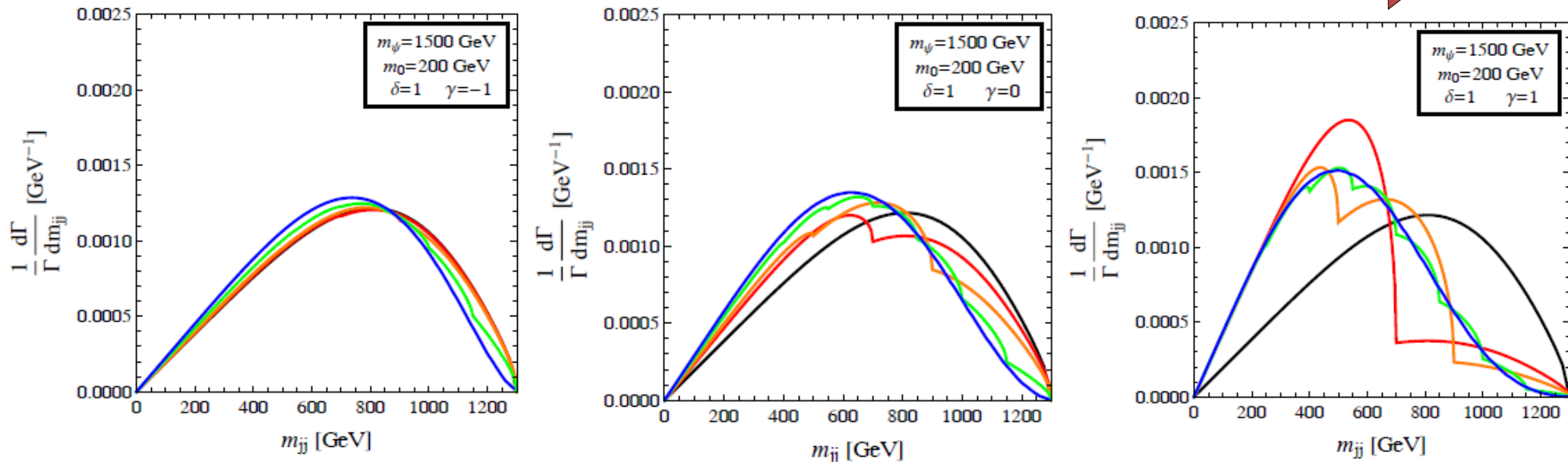


Density of states decreases with n .

Density of states increases with n .

DDM Ensembles & Kinematic Distributions

- Evidence of a DDM ensemble can be ascertained from characteristic features imprinted on the kinematic distributions of these SM particles.

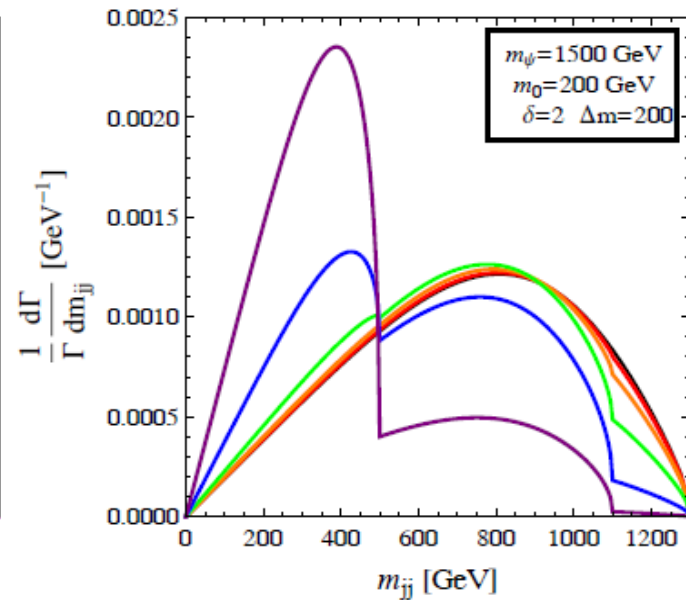
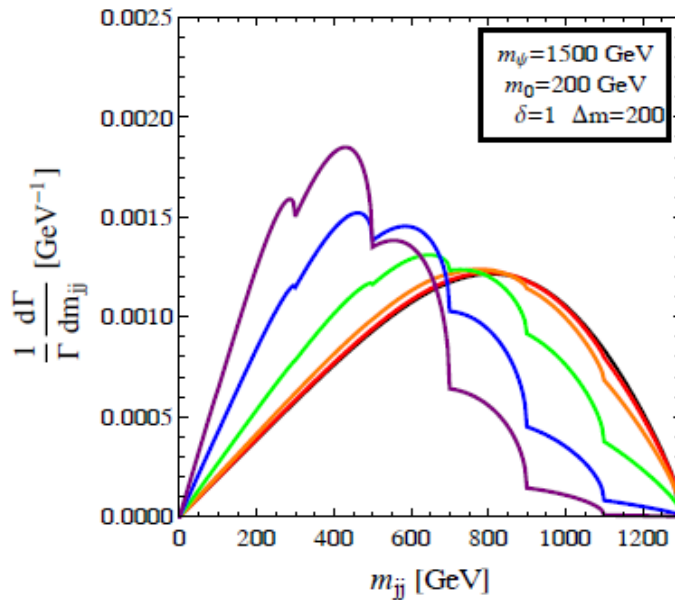
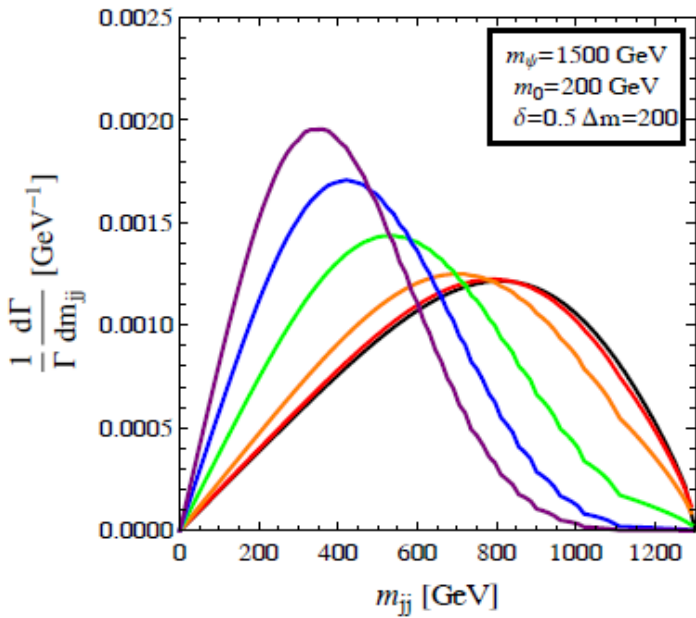


- $\Delta m = 600$ GeV
- $\Delta m = 400$ GeV
- $\Delta m = 150$ GeV
- $\Delta m = 20$ GeV
- $m_\chi = m_0$

- For example, in the scenarios we're considering here, the (normalized) dijet invariant-mass distribution is given by

$$\frac{1}{\Gamma_\psi} \frac{d\Gamma_\psi}{dm_{jj}} = \sum_{n=0}^{n_{\max}} \left(\frac{1}{\Gamma_{\psi n}} \frac{d\Gamma_{\psi n}}{dm_{jj}} \times \text{BR}_{\psi n} \right)$$

Increasing δ



- $\gamma = -2$
- $\gamma = -1$
- $\gamma = 0$
- $\gamma = 1$
- $\gamma = 2$
- $m_\chi = m_0$

Two Characteristic Signatures:

1.

Multiple distinguishable peaks

Large δ , Δm : individual contributions from two or more of the χ_n can be resolved.

2.

The Collective Bell

Small δ , Δm : Individual peaks cannot be distinguished, mass edge “lost,” m_{jj} distribution assumes a characteristic shape.

But the REAL question is...

How well can we distinguish these features in practice?

In other words: to what degree are the characteristic kinematic distributions to which DDM ensembles give rise truly **distinctive**, in the sense that they cannot be reproduced by **any** traditional DM model?

The Procedure:

- Survey over traditional DM models with different DM-candidate masses m_χ and coupling structures.
- Divide the into bins with width determined by the invariant-mass resolution Δm_{jj} of the detector (dominated by jet-energy resolution ΔE_j).
- For each value of m_χ in the survey, define a χ^2 statistic $\chi^2(m_\chi)$ to quantify the degree to which the two resulting m_{jj} distributions differ.


$$\chi^2(m_\chi) = \sum_k \frac{[X_k - \mathcal{E}_k(m_\chi)]^2}{\sigma_k^2}$$

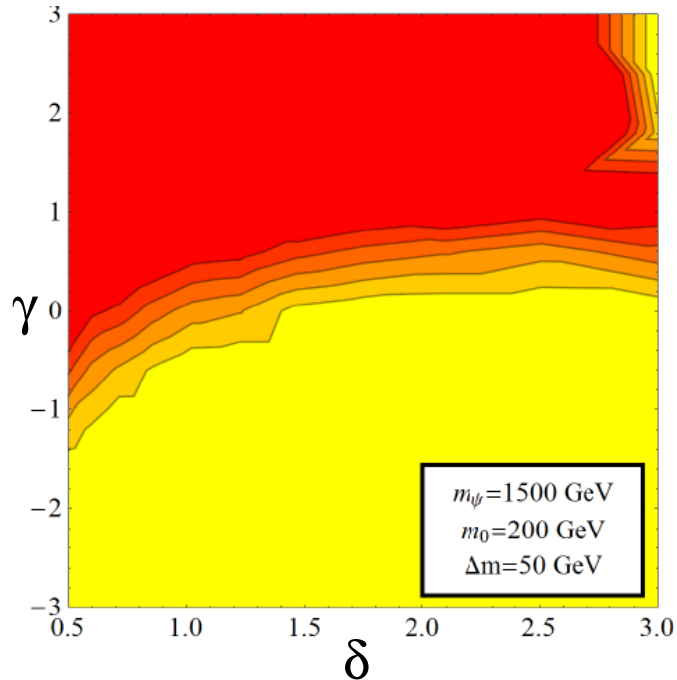

$$\chi_{\min}^2 = \min_{m_\chi} \{ \chi^2(m_\chi) \}$$

- The **minimum** χ^2 value from among these represents the degree to which a DDM ensemble can be distinguished from **any** traditional DM candidate.

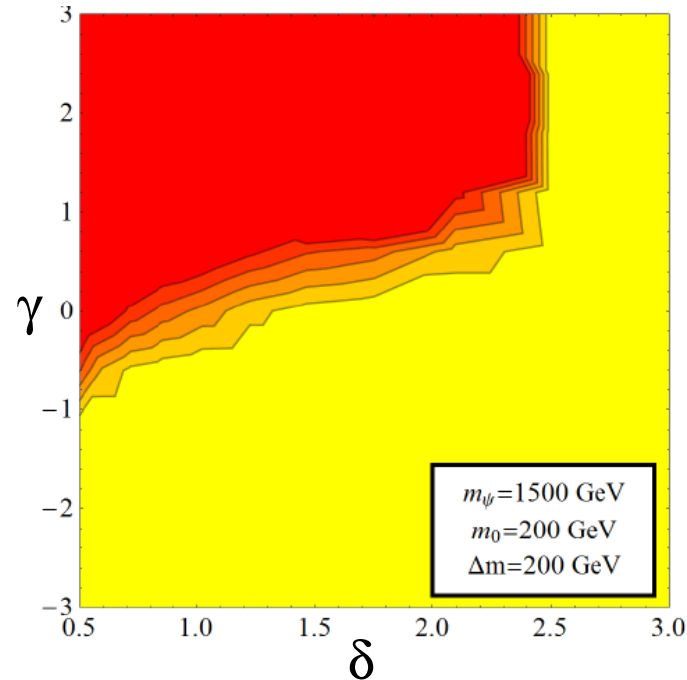
Distinguishing DDM Ensembles: Results

Results for $N_e = 1000$ signal events (e.g., $pp \rightarrow \psi\psi$ for TeV-scale parent, $L_{\text{int}} < 30 \text{ fb}^{-1}$)

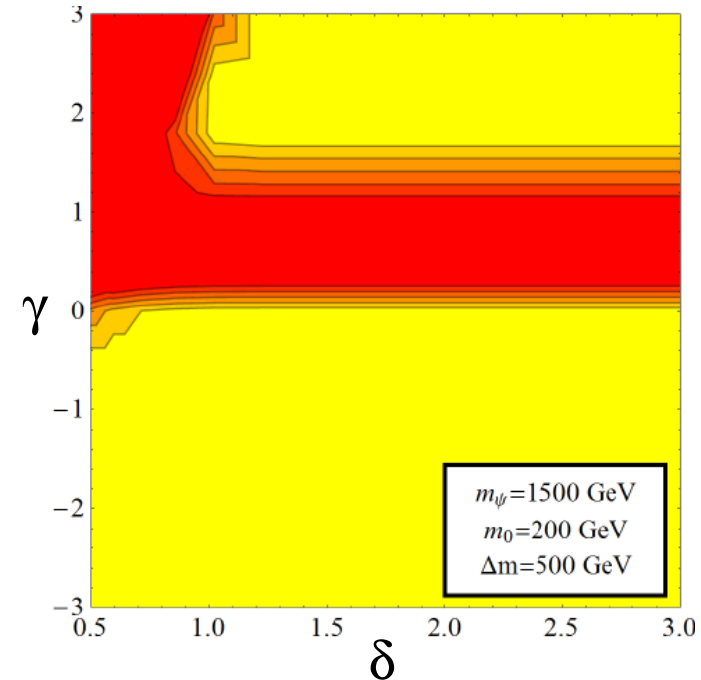
$\Delta m = 50 \text{ GeV}$



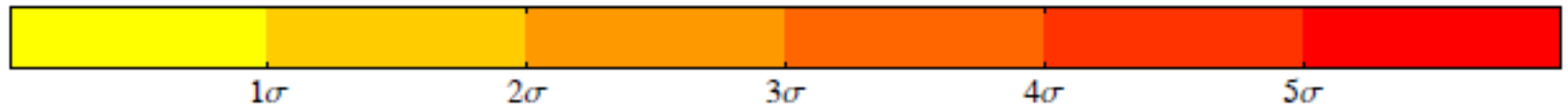
$\Delta m = 200 \text{ GeV}$



$\Delta m = 500 \text{ GeV}$



Significance:



The Main Message:

DDM ensembles can be distinguished from traditional DM candidates at the 5σ level throughout a substantial region of parameter space.

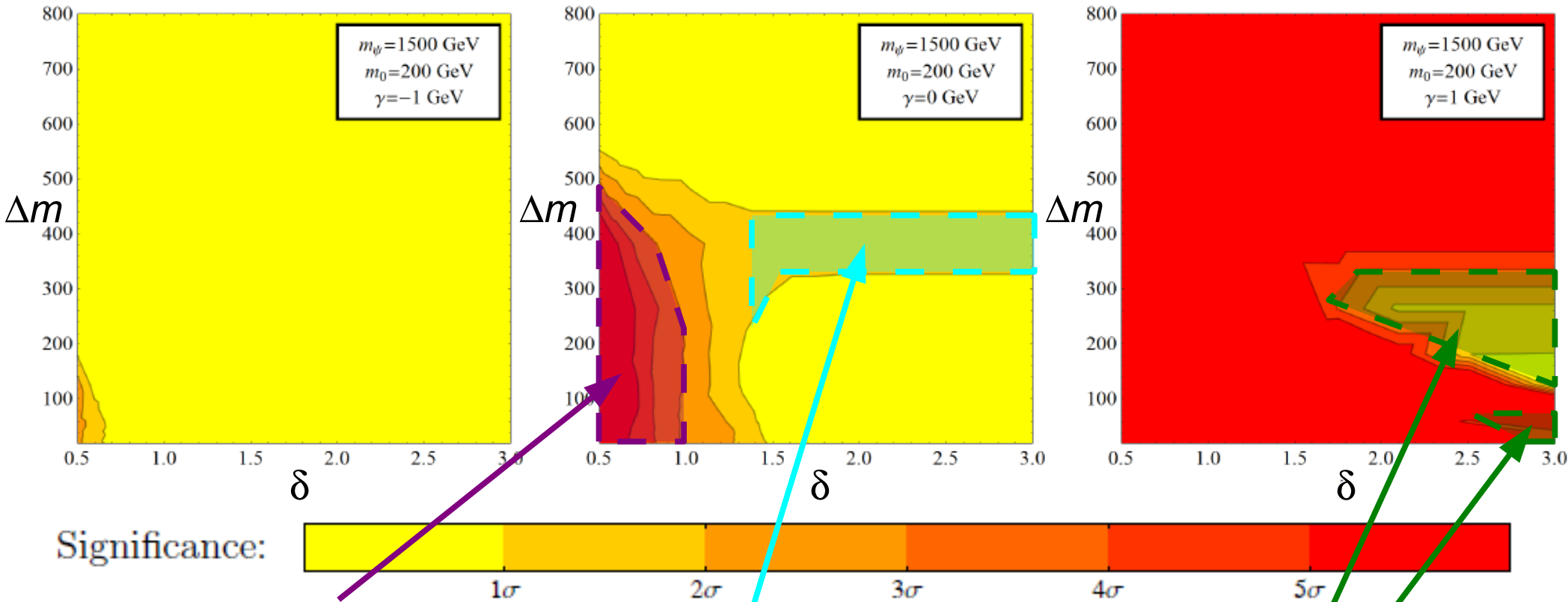
Distinguishing DDM Ensembles: Results

Results for $N_e = 1000$ signal events (e.g., $pp \rightarrow \psi\psi$ for TeV-scale parent, $L_{\text{int}} < 30 \text{ fb}^{-1}$)

$$\gamma = -1$$

$$\gamma = 0$$

$$\gamma = 1$$



Large number of states accessible for small Δm , δ

$\text{BR}(\psi \rightarrow jj\chi_0) \approx \text{BR}(\psi \rightarrow jj\chi_1)$:
two distinct m_{jj} peaks.

Only χ_0 and χ_1 kinematically accessible. One or the other dominates the width of ψ .

A large, circular detector array, likely a Superconducting Tunnel Junction (STJ) array, is shown. It consists of a central hub with numerous small, square detector elements arranged in a grid pattern. The elements are dark in color, possibly black or dark grey, and are mounted on a light-colored, possibly white or light blue, substrate. The array is viewed from a slightly elevated angle, showing its circular shape and the spacing between the elements. The background is a plain, light-colored surface.

Distinguishing DDM at Direct-Detection Experiments

Direct Detection of DDM

- Direct-detection experiments offer another possible method for distinguishing DDM ensembles from traditional DM candidates.
- After the initial observation an excess of signal events at such an experiment, the shape of the **recoil-energy spectrum** associated with those events can provide additional information about the properties of the DM candidate.
- A number of factors impact the shape of the recoil-energy spectrum in a generic dark-matter scenario. **Particle physics**, **astrophysics**, and **cosmology** all play an important role.

The diagram illustrates the equation for the recoil energy spectrum, $\frac{dR}{dE_R} = \sum_j \frac{\sigma_{Nj}^{(0)}}{2m_j \mu_{Nj}^2} F^2(E_R) \rho_j^{\text{loc}} \int_{v_{\text{min}}^{(j)}}^{v_{\text{esc}}} \frac{f_j(v)}{v} dv$, with various components annotated:

- Particle physics:** $\sigma_{Nj}^{(0)}$ is labeled as χ_j -nucleus scattering cross-section. $2m_j \mu_{Nj}^2$ is labeled as the reduced mass of the χ_j -nucleon system.
- Nuclear physics:** $F^2(E_R)$ is labeled as the Form factor.
- Astrophysics and cosmology:** ρ_j^{loc} is labeled as the Local energy density of χ_j . The integral term $\int_{v_{\text{min}}^{(j)}}^{v_{\text{esc}}} \frac{f_j(v)}{v} dv$ is labeled as the Halo-velocity distribution for χ_j .

Direct Detection of DDM

In this talk, I'll adopt the following standard assumptions about the particles in the DM halo as a definition of the “**standard picture**” of DM:

- Total local DM energy density: $\rho_{\text{tot}}^{\text{loc}} \approx 0.3 \text{ GeV}/\text{cm}^3$.
- Maxwellian distribution of halo velocities for all χ_j .
- Local circular velocity $v_0 \approx 220 \text{ km/s}$, galactic escape velocity $v_e \approx 540 \text{ km/s}$.
- Woods-Saxon form factor.
- Spin-independent (SI) scattering dominates.
- Isospin conservation: $f_{pj} = f_{nj}$.
- Local DM abundance \propto global DM abundance: $\rho_j^{\text{loc}} / \rho_{\text{tot}}^{\text{loc}} \approx \Omega_j / \Omega_{\text{tot}}$.

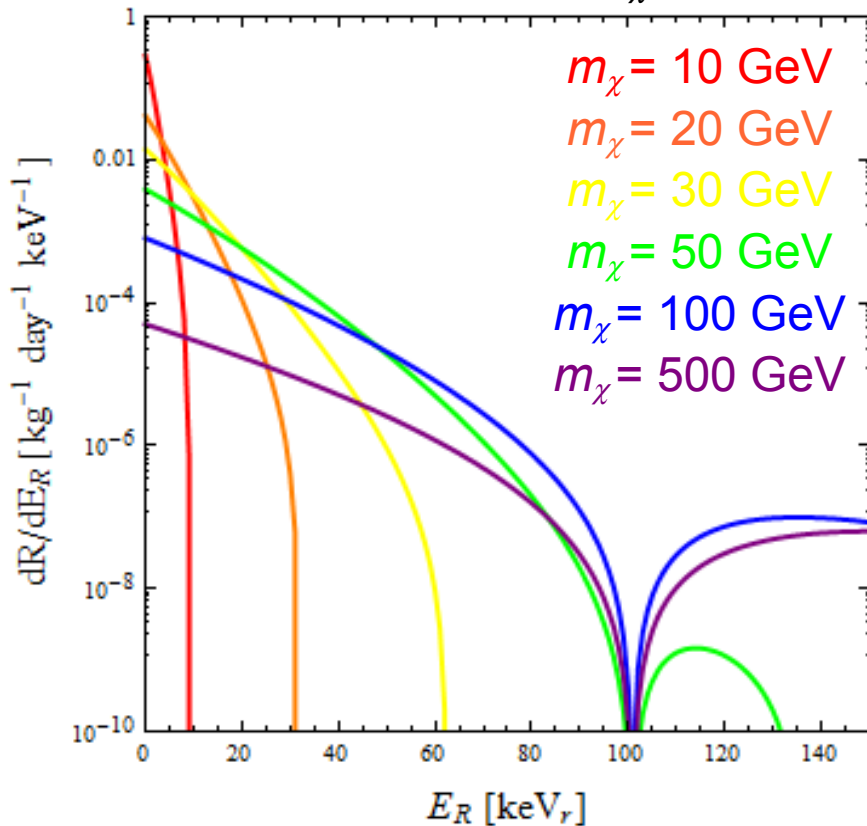
Departures from this standard picture (isospin violation, non-standard velocity distributions, etc.) can have important experimental consequences.

Here, we examine the consequences of replacing a traditional DM candidate with a DDM ensemble, with all other things held fixed.

Recoil-Energy Spectra: Traditional DM

- Let's begin by reviewing the result for the spin-independent scattering of a traditional DM candidate χ off a an atomic nucleus N with mass m_N .
- Recoil rate exponentially suppressed for $E_R \gtrsim 2m_\chi^2 m_N v_0^2 / (m_\chi + m_N)^2$

Target material: Xe
Normalization: $\sigma_{N\chi} = 1$ pb



Two Mass Regimes:

Low-mass regime: $m_\chi \lesssim 20 - 30$ GeV

Spectrum sharply peaked at low E_R due to velocity distribution. Shape quite sensitive to m_χ .

High-mass regime: $m_\chi \gtrsim 20 - 30$ GeV

Broad spectrum. Shape not particularly sensitive to m_χ .

Form-factor
effect

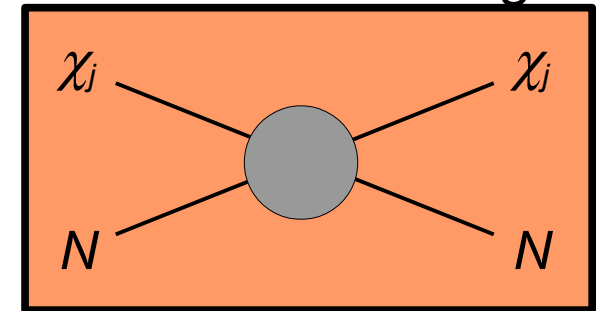
DDM Ensembles and Particle Physics

- Cross-sections depend on effective couplings between the χ_j and nuclei.
- Both **elastic and inelastic scattering** can in principle contribute significantly to the total SI scattering rate for a DDM ensemble.
- In this talk, I'll focus on elastic scattering: $\chi_j N \rightarrow \chi_j N$.
- For concreteness, I'll focus on the case where the couplings between the χ_j and nucleons scale like:

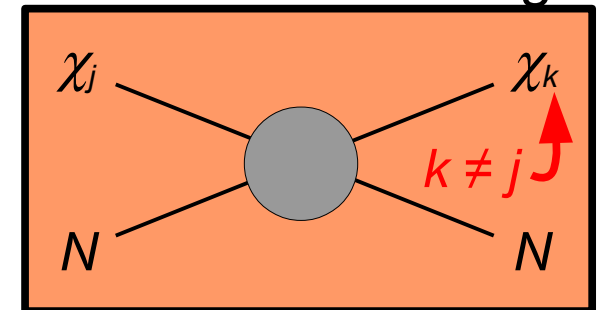
$$f_{nj} = f_{n0} \left(\frac{m_j}{m_0} \right)^\beta \quad \Rightarrow \quad \sigma_{nj}^{(\text{SI})} = \frac{4\mu_{nj}^2}{\pi} f_{nj}^2$$

- However, note that inelastic scattering has special significance within the DDM framework:

Elastic Scattering



Inelastic Scattering



- Possibility of **downscattering** ($m_k < m_j$) as well as upscattering ($m_k > m_j$) within a DDM ensemble.
- Scattering rates for $\chi_j N \rightarrow \chi_k N$ place lower bounds on rates for decays of the form $\chi_j \rightarrow \chi_k + [\text{SM fields}]$ and hence bounds **on the lifetimes** of the χ_j .

DDM Ensembles and Cosmology

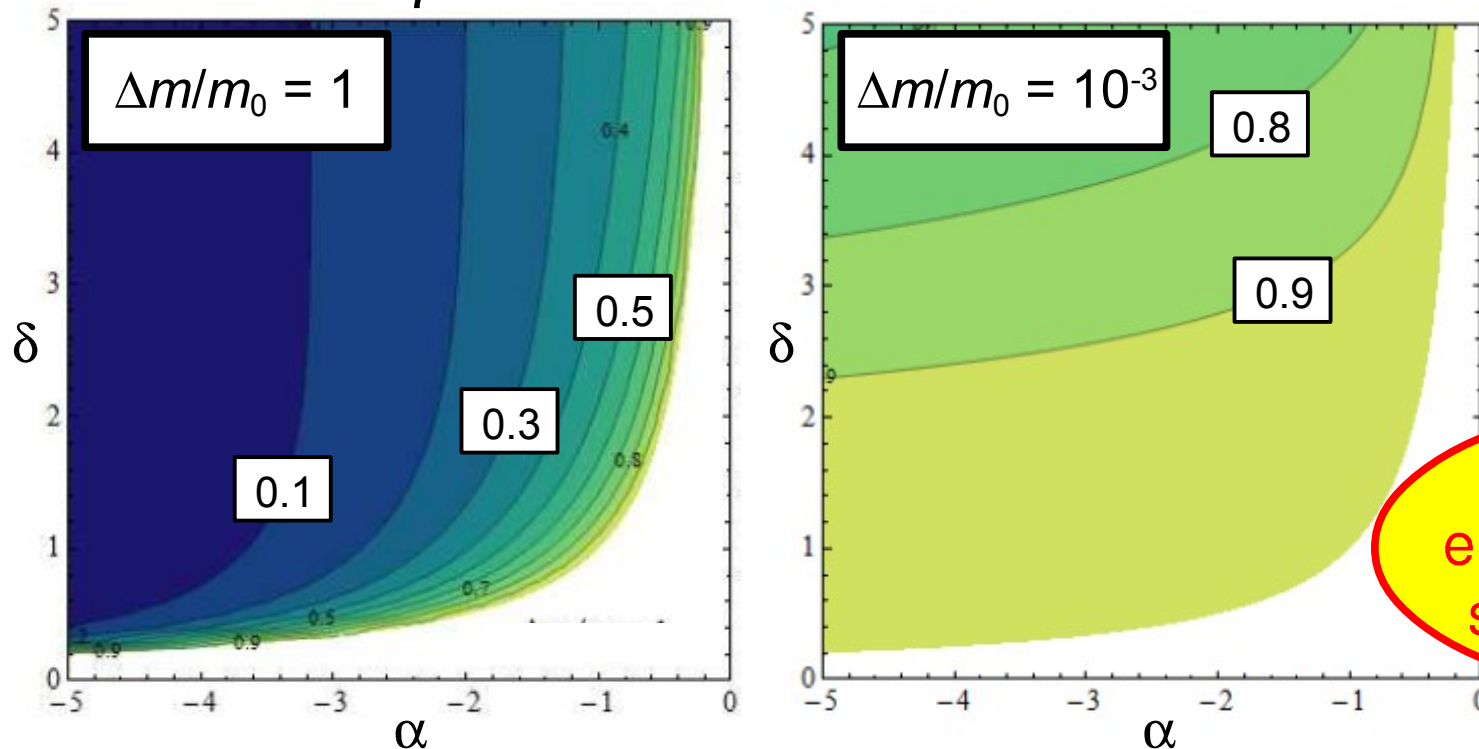
- In contrast to the collider analysis presented above, direct detection involves **a cosmological population** of DM particles, and thus aspects of DDM cosmology.
- Recall that the cosmology of a given DDM ensemble is primarily characterized by the two parameters η and Ω_{tot} .
- For concreteness, consider the case where $m_j = m_0 + n^\delta \Delta m$ and the present-day abundances Ω_j scale like: \longrightarrow

$$\Omega_{\text{tot}} = \sum_j \Omega_j$$

$$\eta = 1 - \frac{\Omega_0}{\Omega_{\text{tot}}}$$

$$\Omega_j = \Omega_0 \left(\frac{m_j}{m_0} \right)^\alpha$$

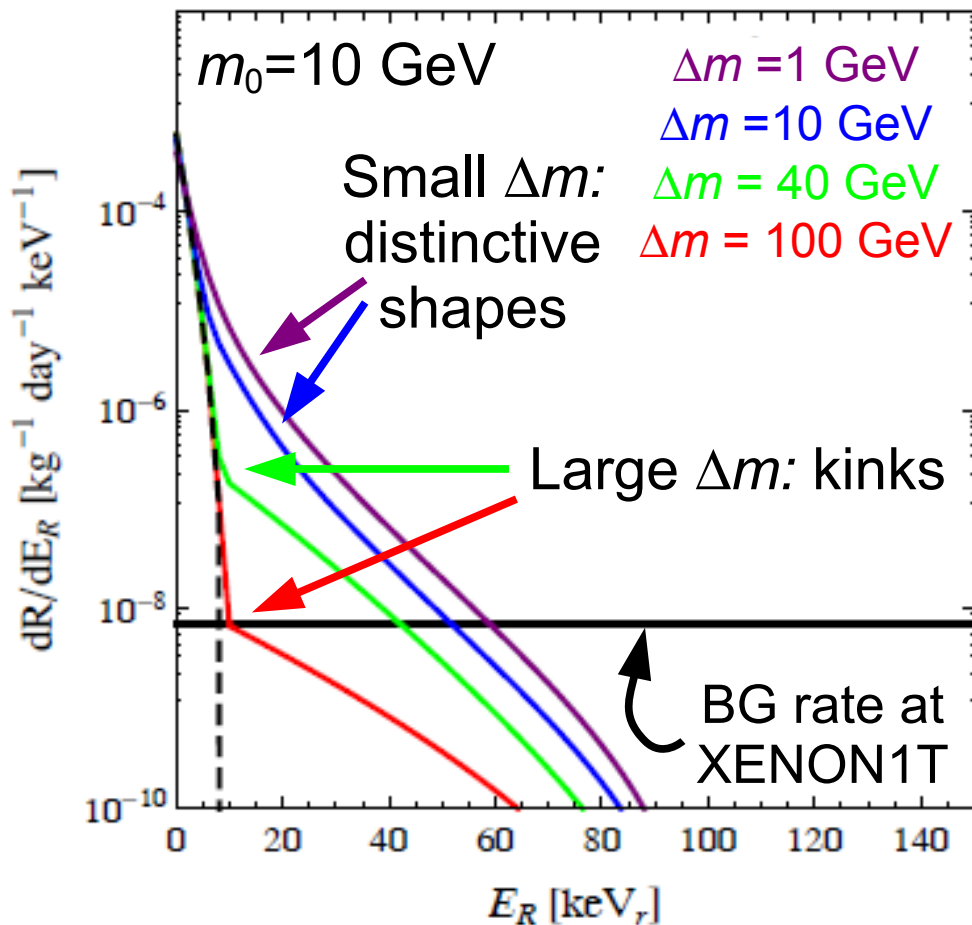
η as a function of α and δ



$\eta \sim \mathcal{O}(1)$: the full ensemble contributes significantly to Ω_{tot} .

Recoil-Energy Spectra: DDM

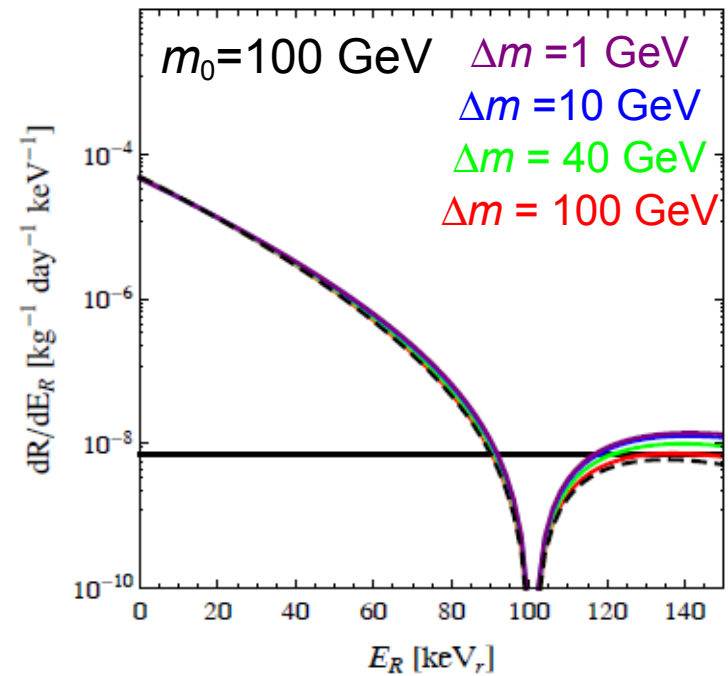
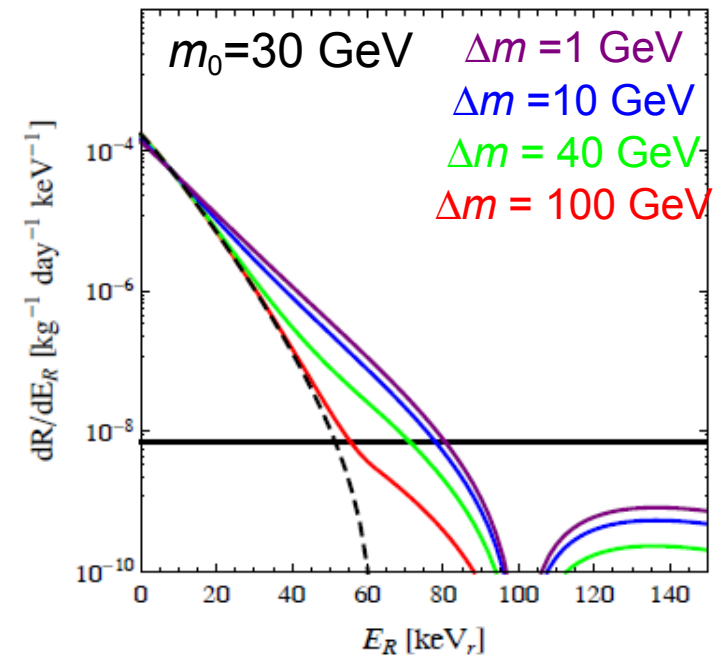
- **Distinctive features** emerge in the recoil-energy spectra of DDM models, especially when one or more of the χ_j are in the low-mass regime.
- As m_0 increases, more of the χ_j shift to the high-mass regime. Spectra increasingly resemble those of traditional DM candidates with $m_\chi \approx m_0$.



$\alpha = -1.5$
 $\beta = -1$
 $\delta = 1$

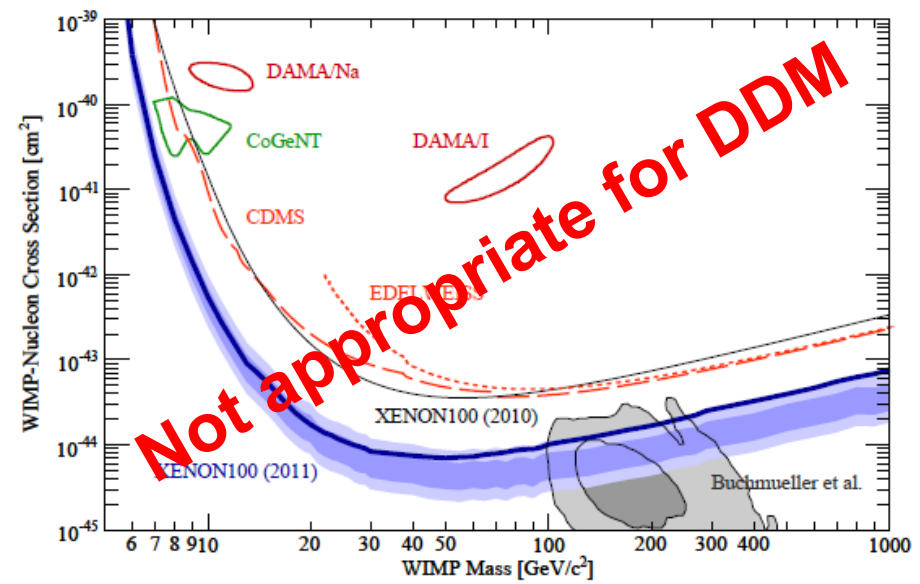
Xe target

Rate normalized to that of χ with $\sigma_\chi^{(\text{SI})} = 10^{-9} \text{ pb}$

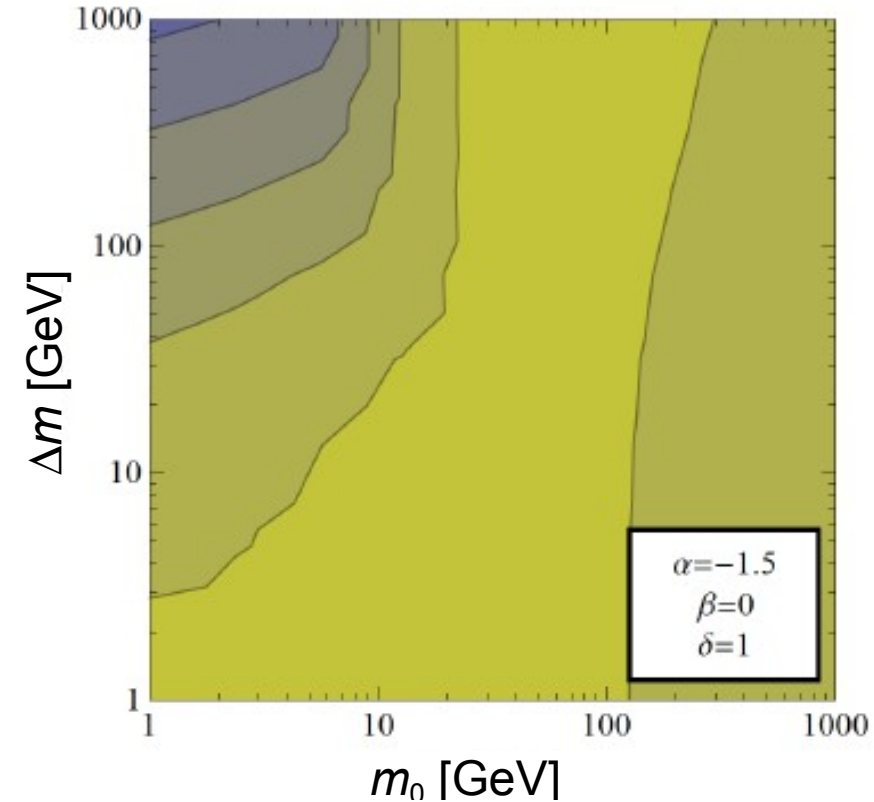
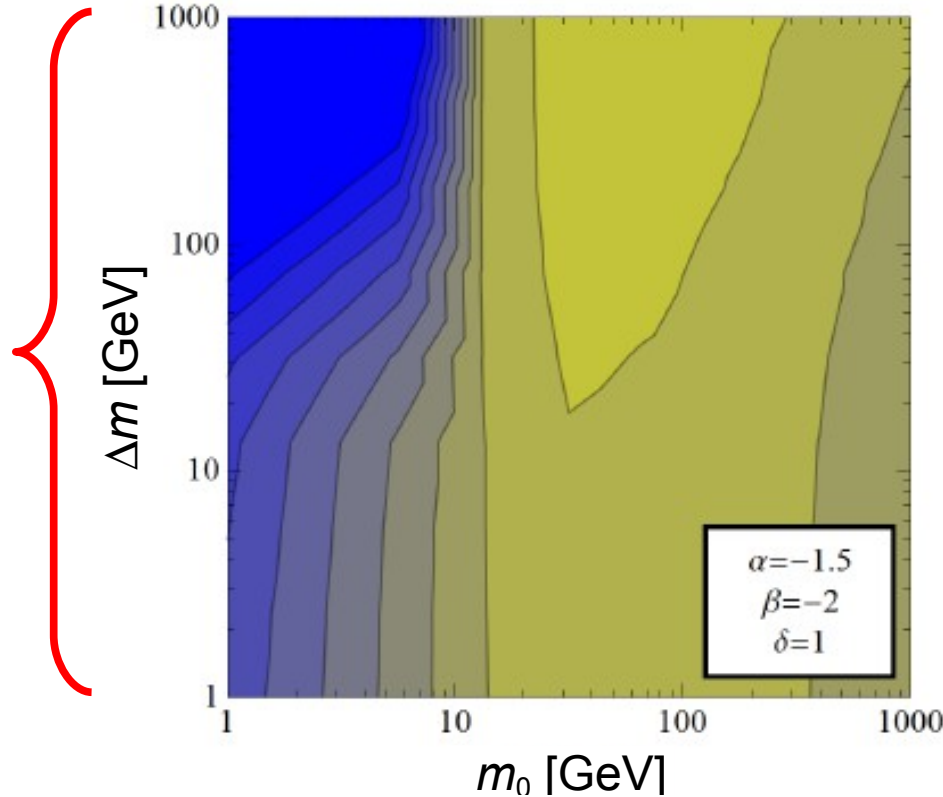


Constraining Ensembles:

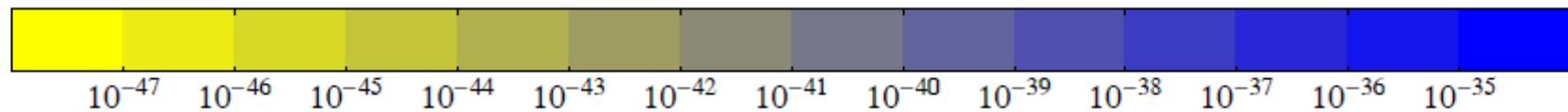
- Experimental limits constrain DDM models just as they constrain traditional DM models.
- A DDM ensemble has no well-defined mass or interaction cross-section: limits *cannot* be phrased as bounds on m_χ and $\sigma_\chi^{(SI)}$.
- Most stringent limits from XENON100 data.



Bounds
on χ_0
 $\sigma_{n0}^{(SI)}$ in
DDM
models:



$\sigma_{n0,max}^{(SI)} [cm^{-2}] :$



How well can we distinguish a departure from the standard picture of DM due to the presence of a DDM ensemble on the basis of direct-detection data?

Consider the case in which a *particular* experiment, characterized by certain attributes including...

Target material(s)
Detection method

Fiducial Volume
Data-collection time

Signal acceptance
Recoil-energy window

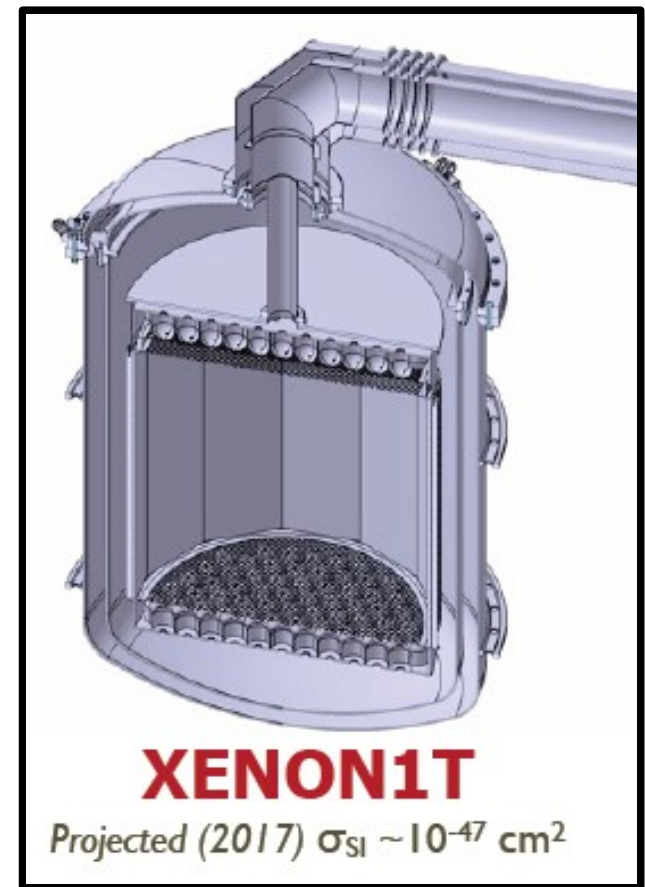
...reports a statistically significant excess in the number of signal events.

The Procedure (much like in our collider analysis):

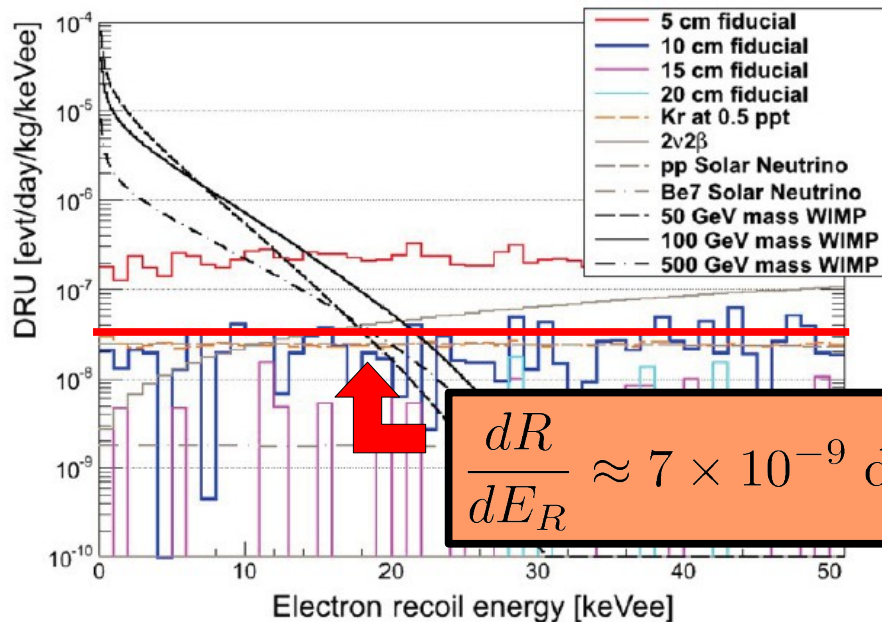
- Compare the recoil-energy spectrum for a given DDM ensemble to those of traditional DM candidates which yield the **same total event rate** at a given detector.
- Survey over traditional DM candidates with different m_χ and define a χ^2 statistic for each m_χ to quantify the degree to which the corresponding recoil-energy spectrum differs from that associated with the DDM ensemble.
- The minimum χ^2_{\min} of these quantifies the degree to which the DDM model can be distinguished from traditional DM candidates, under standard astrophysical assumptions.

As an example, consider a detector with similar attributes to those anticipated for the next generation of noble-liquid experiments (XENON1T, LUX/LZ, PANDA-X, et al.). In particular, we take:

- Liquid-xenon target
- Fiducial volume ~ 5000 kg
- Five live years of operation.
- Energy resolution similar to XENON100
- Acceptance window: $8 \text{ keV} < E_R < 48 \text{ keV}$

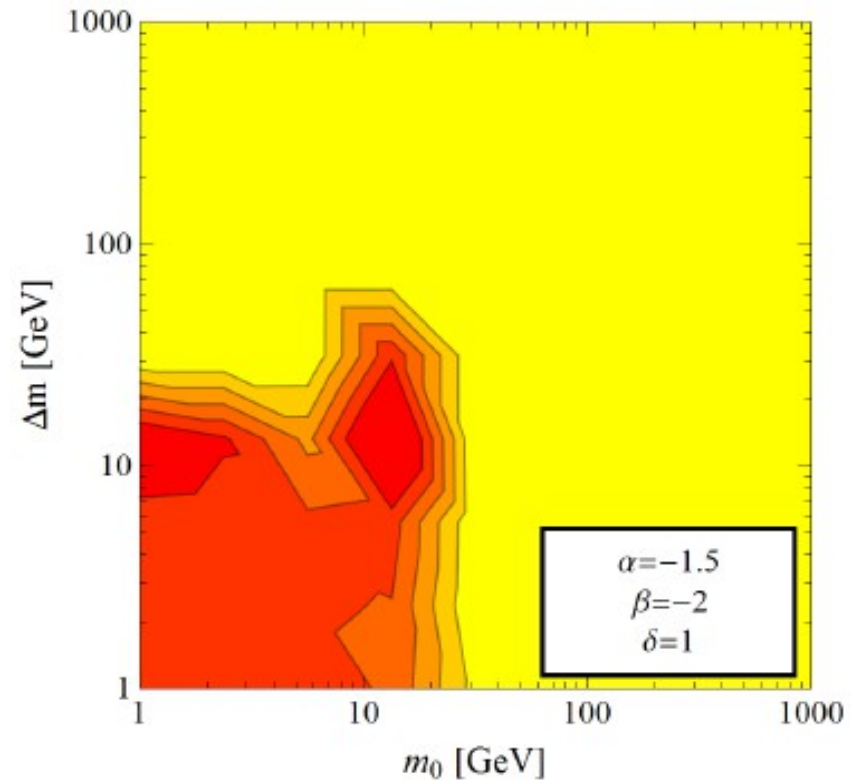
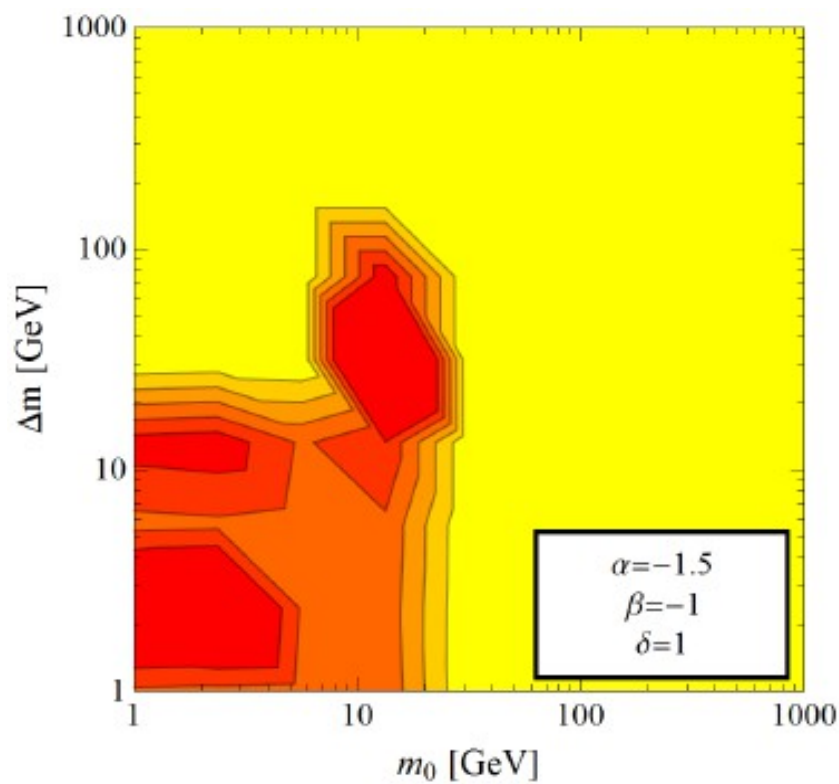


Background Contribution

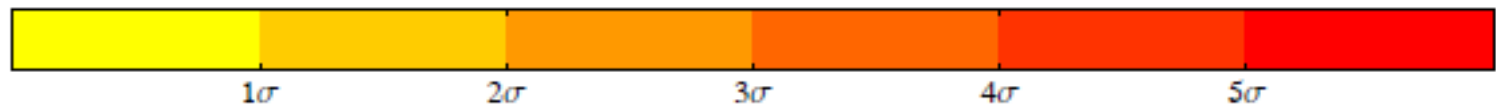


- $N_e \sim 1000$ total signal events observed (consistent with most stringent current limits from XENON100).
- Background dR/dE_R spectrum essentially flat

Distinguishing DDM Ensembles: Results



Significance:



The upshot:

In a variety of situations, it should be possible to distinguish characteristic features to which DDM ensembles give rise at the next generation of direct-detection experiments.

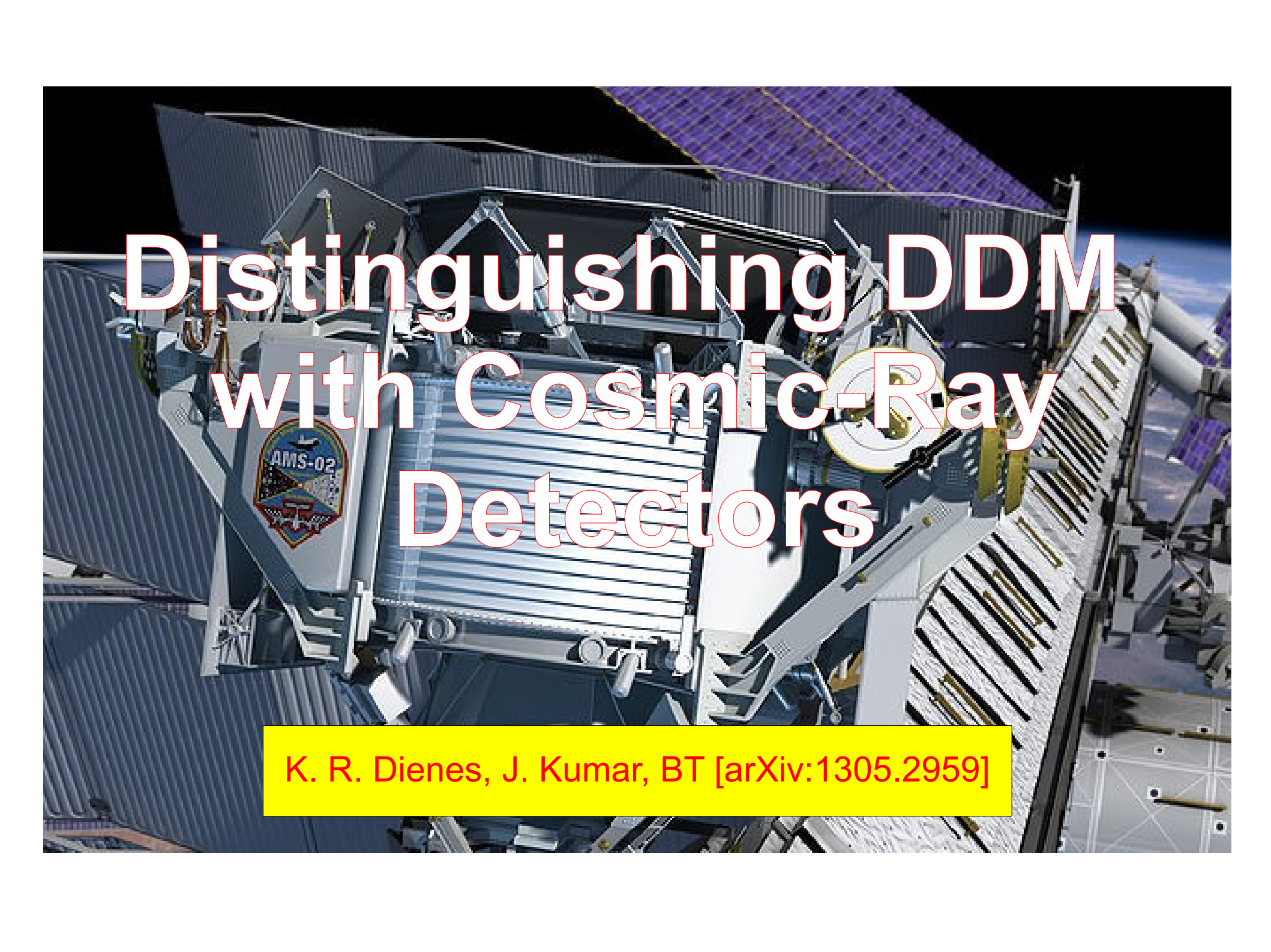
- The best prospects are obtained in cases where multiple χ_j are in the low-mass regime: $m_j \lesssim 30$ GeV.
- A 5σ significance of differentiation is also possible in cases in which only χ_0 is in the low-mass regime and a kink in the spectrum can be resolved.

CAUTION

Discrepancies in recoil-energy spectra from standard expectations can arise due to several other factors as well (complicated halo-velocity distribution, velocity-dependent interactions, etc.). Care should be taken in interpreting such discrepancies in the context of any particular model.

However,

By comparing/correlating signals from **multiple experiments** it should be possible to distinguish between a DDM interpretation and many of these alternative possibilities.

A detailed 3D rendering of the Alpha Magnetic Spectrometer (AMS-02) detector, a particle physics experiment, mounted on the International Space Station. The detector is a complex structure of white and grey metal frames, with various components and sensors visible. A prominent feature is a large, circular, gold-colored component. The background shows the dark blue and black of space, with the Earth's horizon and some of the station's structure visible. The text "Distinguishing DDM with Cosmic-Ray Detectors" is overlaid in large, white, outlined letters.

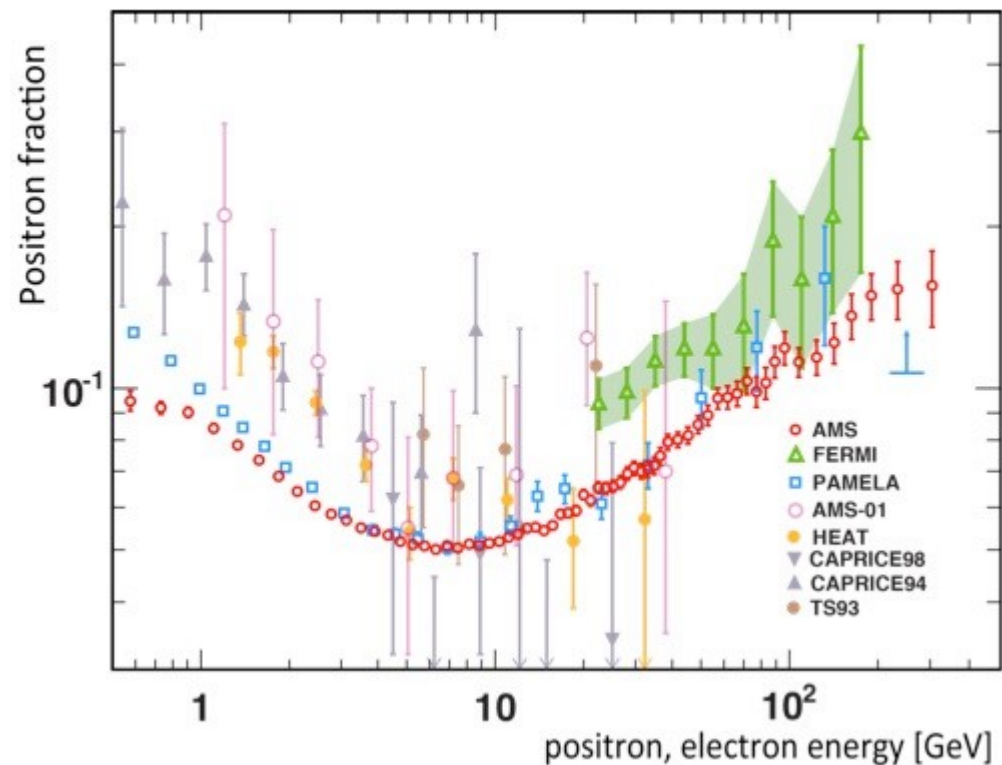
Distinguishing DDM with Cosmic-Ray Detectors

K. R. Dienes, J. Kumar, BT [arXiv:1305.2959]

The Positron Puzzle

PAMELA, AMS-02, and a host of other experiments have reported an excess of cosmic-ray positrons.

Annihilating or decaying dark-matter in the galactic halo has been advanced as a possible explanation of this data anomaly.



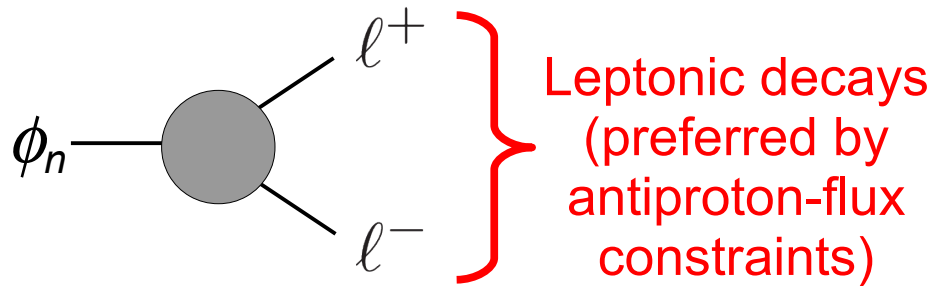
Dark-matter candidates whose annihilations or decays reproduce the observed positron fraction typically run into other issues:

- Limits on the continuum gamma-ray flux from FERMI, etc.
- Limits on the cosmic-ray antiproton flux from PAMELA, etc.
- Cannot simultaneously reproduce the total e^\pm flux from FERMI, etc.
- Leave imprints in the CMB not observed by WMAP/PLANCK.

DDM ensembles can actually go a long way toward reconciling these tensions.

DDM Ensembles and Cosmic Rays

For concreteness, consider the case in which the ensemble constituents ϕ_n are scalar fields which couple to pairs of SM fermions.



$$l^\pm = \{e^\pm, \mu^\pm, \tau^\pm\}$$

Provides best fit to combined e^\pm flux.

e.g.,
$$\mathcal{L}_{\text{int}} = \frac{c_n}{\Lambda} (\partial_\mu \phi_n) \bar{l} \gamma^\mu l$$

Parametrizing the ensemble

Masses:

$$m_n = m_0 + n^\delta \Delta m$$

Couplings:

$$c_n = c_0 \left(\frac{m_n}{m_0} \right)^\xi$$

Abundances:

$$\Omega_n = \Omega_0 \left(\frac{m_n}{m_0} \right)^\alpha$$

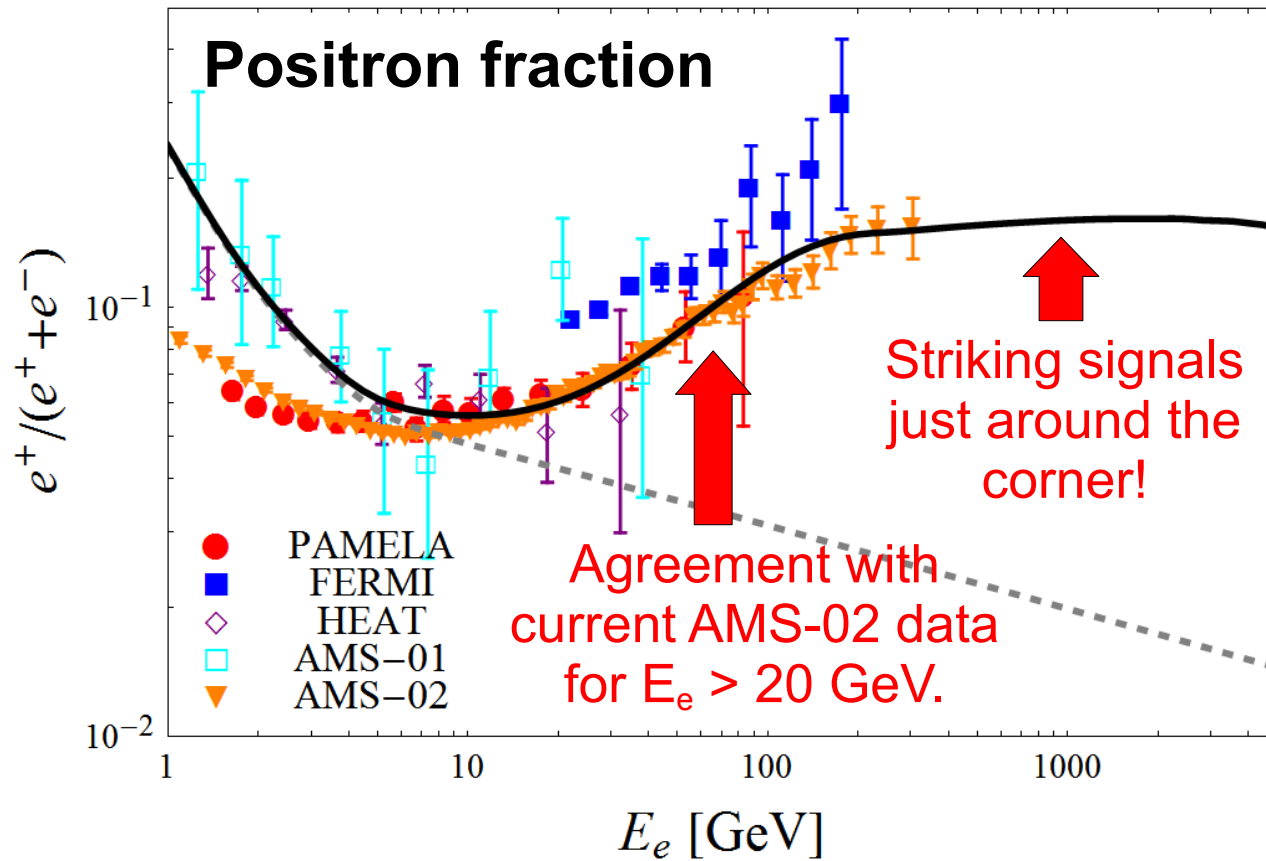
Distributing the dark-matter relic abundance across the ensemble yields a spectrum of lepton injection energies

Effectively softens the e^\pm spectrum

$$\Gamma_n \sim \frac{m_\ell^2 m_0}{\Lambda^2} \left(\frac{m_n}{m_0} \right)^\gamma$$

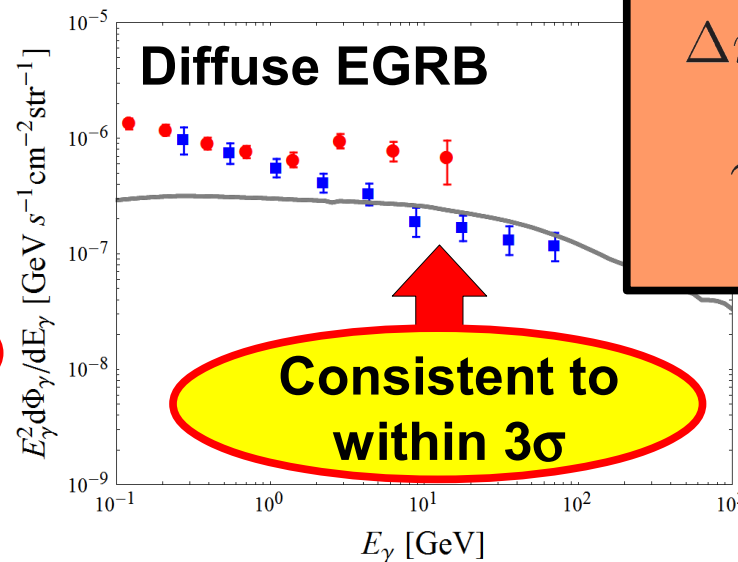
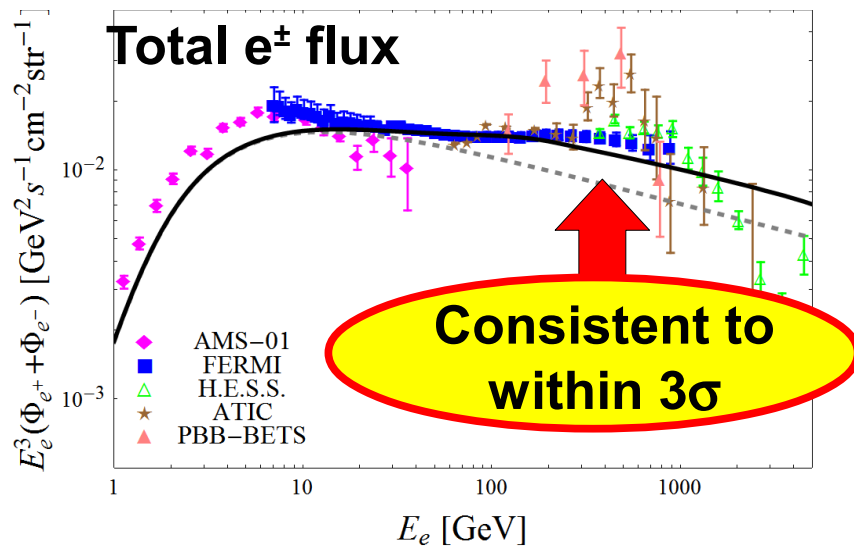
where $\gamma \equiv 1 + 2\xi$

Turndown



Due to this softening, DDM ensembles can reproduce current AMS-02 data while at the same time satisfying gamma-ray constraints.

Ensembles which do this typically also yield striking features – **plateaus** or **soft turn-downs** – in the positron fraction at higher energies.



$m_0 = 500$ GeV
 $\Delta m = 1$ GeV
 $\alpha = -2$
 $\gamma = 0.875$
 $\delta = 1$

Summary

DDM is an alternative framework for dark-matter physics in which stability is replaced by a balancing between lifetimes and abundances across a vast ensemble of particles which collectively account for Ω_{CDM} .

Such DDM ensembles give rise to distinctive experimental signatures which can serve to distinguish them from traditional dark-matter candidates. These include:

- Imprints on kinematic distributions of SM particles at colliders.
- Distinctive features in the recoil-energy spectra observed at direct-detection experiments.
- Unusual features in cosmic-ray e^+ and e^- spectra at high energies.

Many more phenomenological handles on DDM and on non-minimal dark sectors in general remain to be explored!

Summary

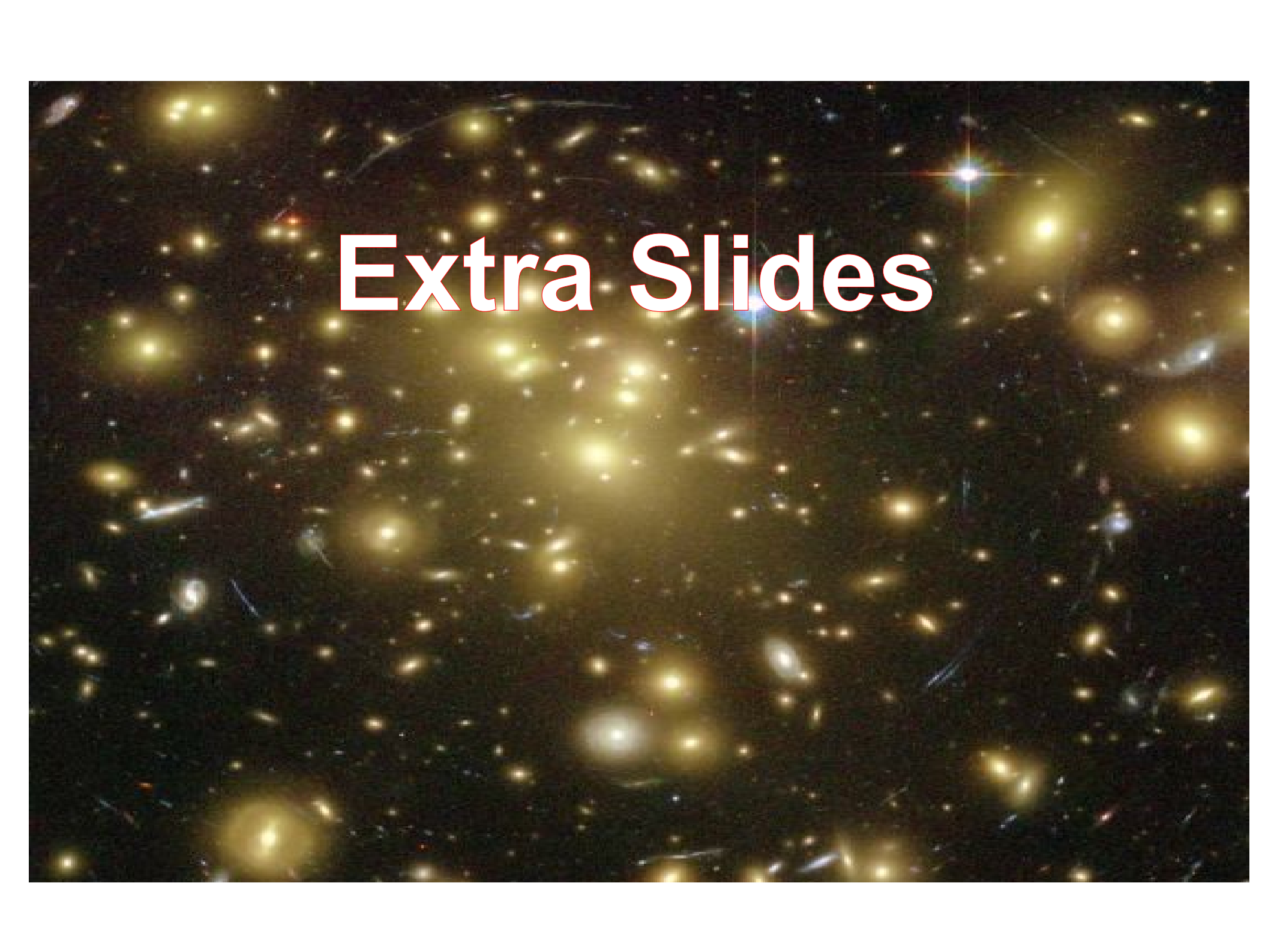
- Dynamical dark matter (DDM) is a new framework for addressing the dark-matter question.
- In this framework, stability is replaced by **a balancing between lifetimes and abundances** across a vast **ensemble** of particles which collectively account for Ω_{CDM} .
- This scenario is well-motivated in string theory and field theory.
- Simple, **explicit models** exist which satisfy all applicable phenomenological constraints.
- DDM ensembles can give rise to **distinctive experimental signatures** at which permit one to distinguish them from traditional dark-matter candidates, including...

- Imprints on kinematic distributions of SM particles at the LHC.
- Distinctive features in the recoil-energy spectra observed at direct-detection experiments.
- And probably many other signatures waiting to be explored.

Possible Extensions

- Other implications for **indirect detection** (photons, neutrinos, etc.)
- **Inelastic scattering** and direct detection
- Other collider signals for other kinds of DDM ensembles?
- What other production mechanisms can naturally lead to the balance between lifetimes and abundances in different DDM models? (Thermal freeze-out? Production from heavy particle decays?)
- The effects of **intra-ensemble decays** (on abundances, halo-velocity distributions, etc.)
- A full BBN analysis (our viable DDM models are still quite conservative – how far can the envelope be pushed?)
- **Structure formation** in DDM cosmologies: multiple decoupling and free-streaming scales. Possible way of addressing small-scale structure issues?
- DDM ensembles in other contexts? Bulk fields in **warped extra dimensions** (completely different KK spectroscopy)? The **string axiverse**?
- Multiple SM-neutral fields in the bulk → multiple species of dark KK tower
- Since DDM leads to a time-varying Ω_{CDM} , this approach might serve as a useful starting point towards addressing the **cosmic coincidence problem**.
- Relationship between dark matter and dark energy?

Clearly, much remains to be explored!



Extra Slides

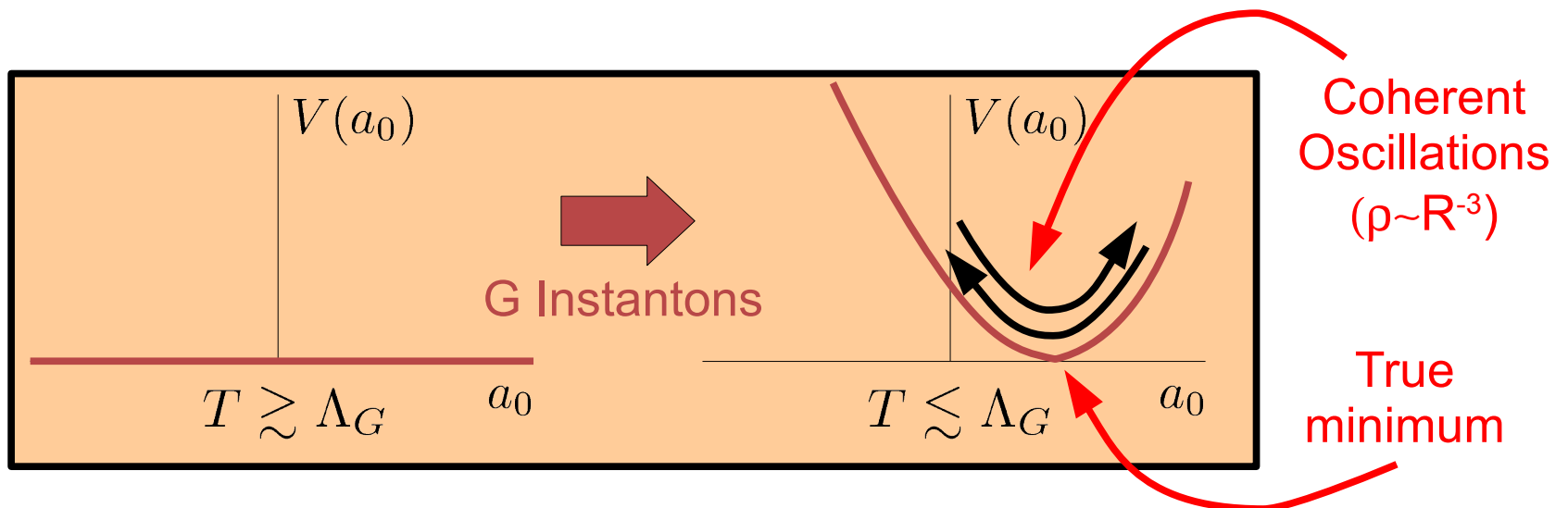
Mixing and Relic Abundances:

- At temperatures $T \gg \Lambda_G$, $m_X \approx 0$. At such temperatures, mixing is negligible, and the potential for a_0 effectively vanishes.
- The expectation value of a_0 at such temperatures is therefore undetermined:

$$\langle a_0 \rangle_{\text{init}} = \theta \hat{f}_X$$

“Misalignment Angle”
(parameterizes initial displacement)

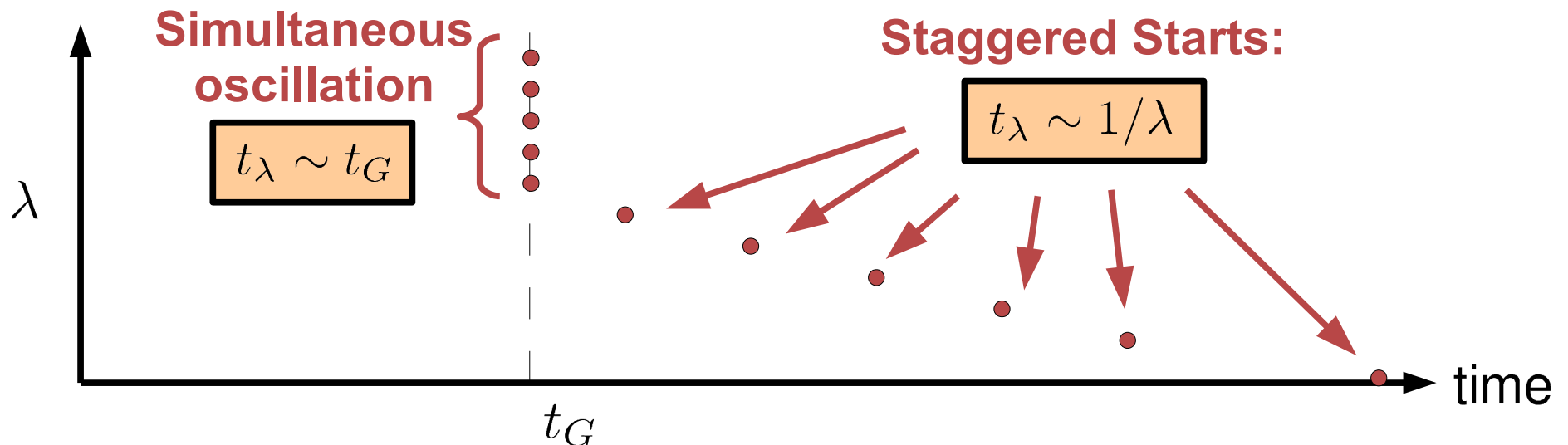
- However, at $T \sim \Lambda_G$, instanton effects turn on:
 - m_X becomes nonzero, so KK eigenstates are no longer mass eigenstates.
 - The zero-mode potential now has a well-defined minimum.



- The a_λ are initially populated (at t_G) according to their overlap with a_0 :

Initial Overlap		Energy Densities
$\langle a_\lambda(t_G) \rangle = \theta \hat{f}_X A_\lambda$	➔	$\rho_\lambda(t_G) = \frac{1}{2} \theta^2 \hat{f}_X^2 \lambda^2 A_\lambda^2$

- Each field begins to oscillate at a time t_λ , when **two** conditions are met:
 1. ρ_λ is nonzero (so $t \gtrsim t_G$).
 2. Mass has become comparable to Hubble Parameter: $\lambda \sim 3H(t)$.
- In the approximation that the instanton potential turns on rapidly, we have two regimes:



Mixing and stability:

- Couplings between SM fields and the a_λ are proportional to $\tilde{\lambda}^2 A_\lambda$.
- This results in a decay-width suppression for modes with $\lambda \lesssim m_X^2/M_c$

The diagram consists of two parts. On the left, a light orange rectangular box contains the equation $\Gamma_\lambda \propto \frac{\lambda^3}{\hat{f}_X^2} (\tilde{\lambda}^2 A_\lambda)^2$. A red arrow points from the $\tilde{\lambda}^2 A_\lambda$ term in the equation to a yellow oval on the right. The oval contains two lines of text: $\mathcal{O}(1)$ for $\lambda \gg \frac{m_X^2}{M_c}$ and Tiny for $\lambda \ll \frac{m_X^2}{M_c}$.

$$\Gamma_\lambda \propto \frac{\lambda^3}{\hat{f}_X^2} (\tilde{\lambda}^2 A_\lambda)^2$$

$\mathcal{O}(1)$ for $\lambda \gg \frac{m_X^2}{M_c}$
Tiny for $\lambda \ll \frac{m_X^2}{M_c}$

- Comparing to the relic-abundance results, above we find that the a_λ with large Γ_λ **automatically** have suppressed Ω_λ !

This balance between Ω_λ and Γ_λ rates relaxes constraints related to:

- Distortions to the CMB
- Features in the diffuse X-ray and gamma-ray background
- Disruptions of BBN
- Late entropy production

The Contribution from Each Field

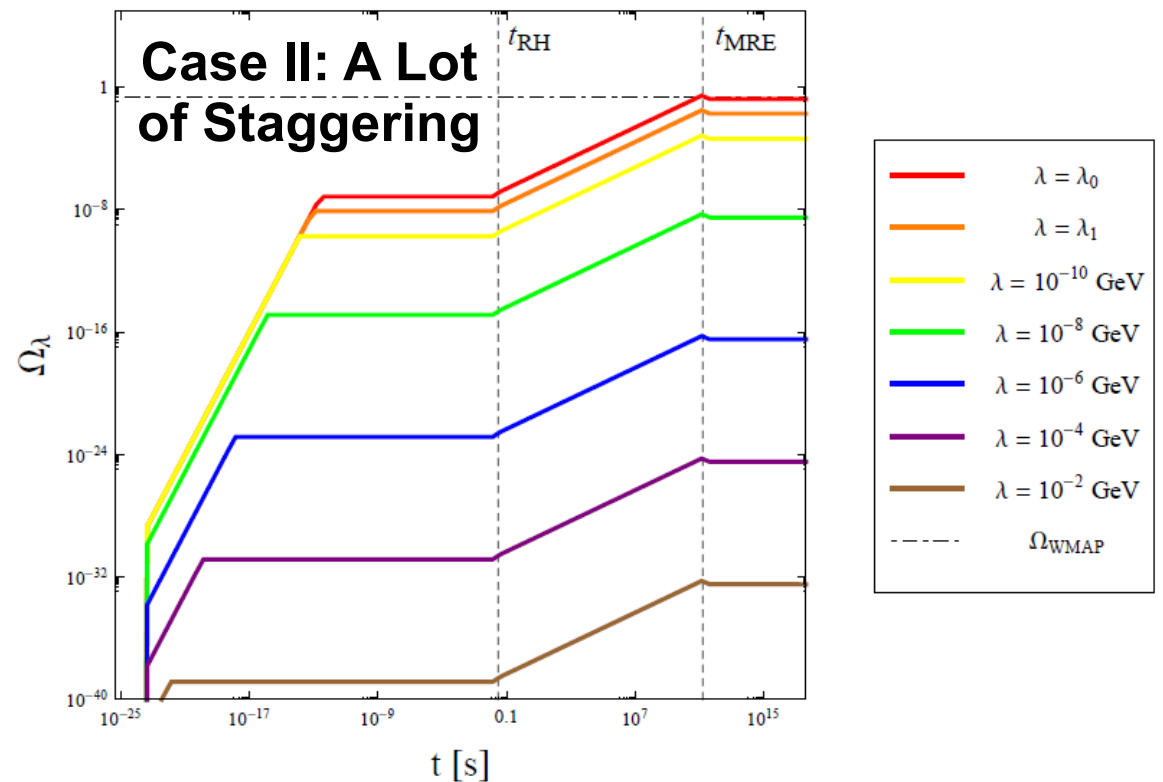
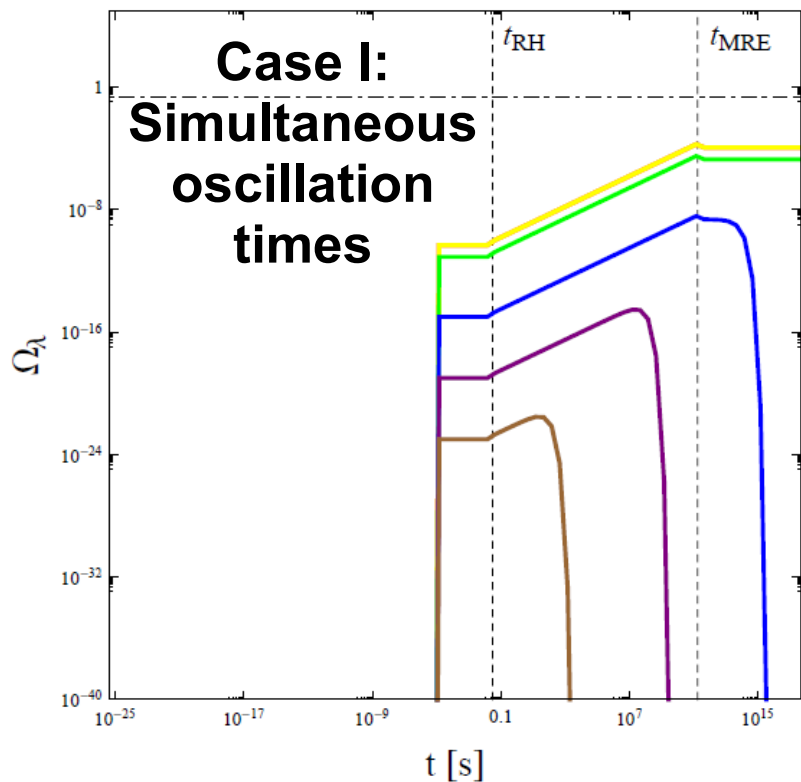
Time-evolution factor
(for t_λ during reheating)

Mixing factor from A_λ^2

Decay suppression

$$\Omega_\lambda = 3 \left(\frac{\theta \hat{f}_X m_X}{M_P} \right)^2 t_\lambda^2 \left[1 + \frac{\lambda^2}{m_X^2} + \frac{\pi^2 m_X^2}{M_c^2} \right]^{-1} e^{-\Gamma_\lambda(t-t_G)} \begin{cases} \frac{1}{4} & 2/\lambda \lesssim t \lesssim t_{\text{RH}} \\ \frac{4}{9} \left(\frac{t}{t_{\text{RH}}} \right)^{1/2} & t_{\text{RH}} \lesssim t \lesssim t_{\text{MRE}} \\ \frac{1}{4} \left(\frac{t_{\text{MRE}}}{t_{\text{RH}}} \right)^{1/2} & t \gtrsim t_{\text{MRE}} \end{cases}$$

t_G^2 (simultaneous) or $4/\lambda^2$ (staggered)



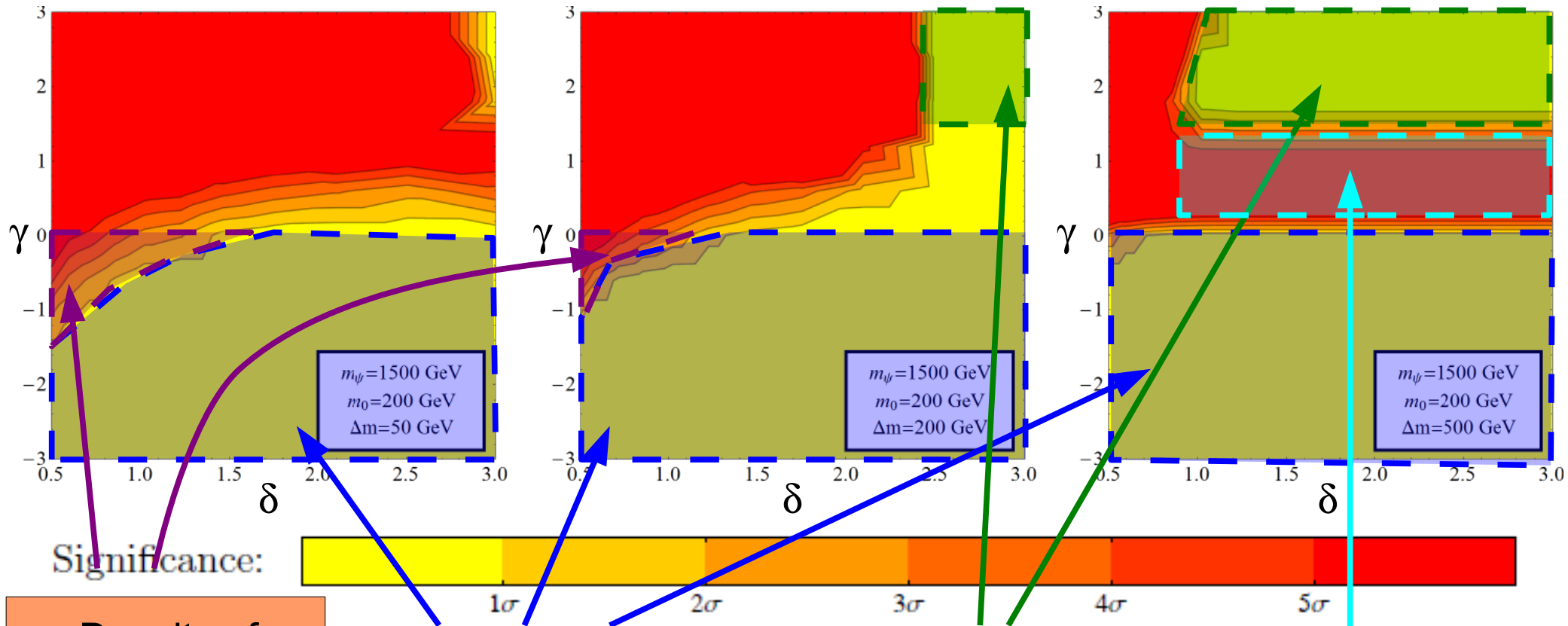
Distinguishing DDM Ensembles: Results

Results for $N_e = 1000$ signal events (e.g., $pp \rightarrow \psi\psi$ for TeV-scale parent, $L_{\text{int}} < 30 \text{ fb}^{-1}$)

$\Delta m = 50 \text{ GeV}$

$\Delta m = 200 \text{ GeV}$

$\Delta m = 500 \text{ GeV}$



$m_\psi = 1500 \text{ GeV}$
 $m_0 = 200 \text{ GeV}$
 $\Delta m = 50 \text{ GeV}$

$m_\psi = 1500 \text{ GeV}$
 $m_0 = 200 \text{ GeV}$
 $\Delta m = 200 \text{ GeV}$

$m_\psi = 1500 \text{ GeV}$
 $m_0 = 200 \text{ GeV}$
 $\Delta m = 500 \text{ GeV}$

Density of states large enough to overcome γ suppression for small δ .

BRs to all χ_n with $n > 1$ suppressed: lightest constituent dominates the width of ψ .

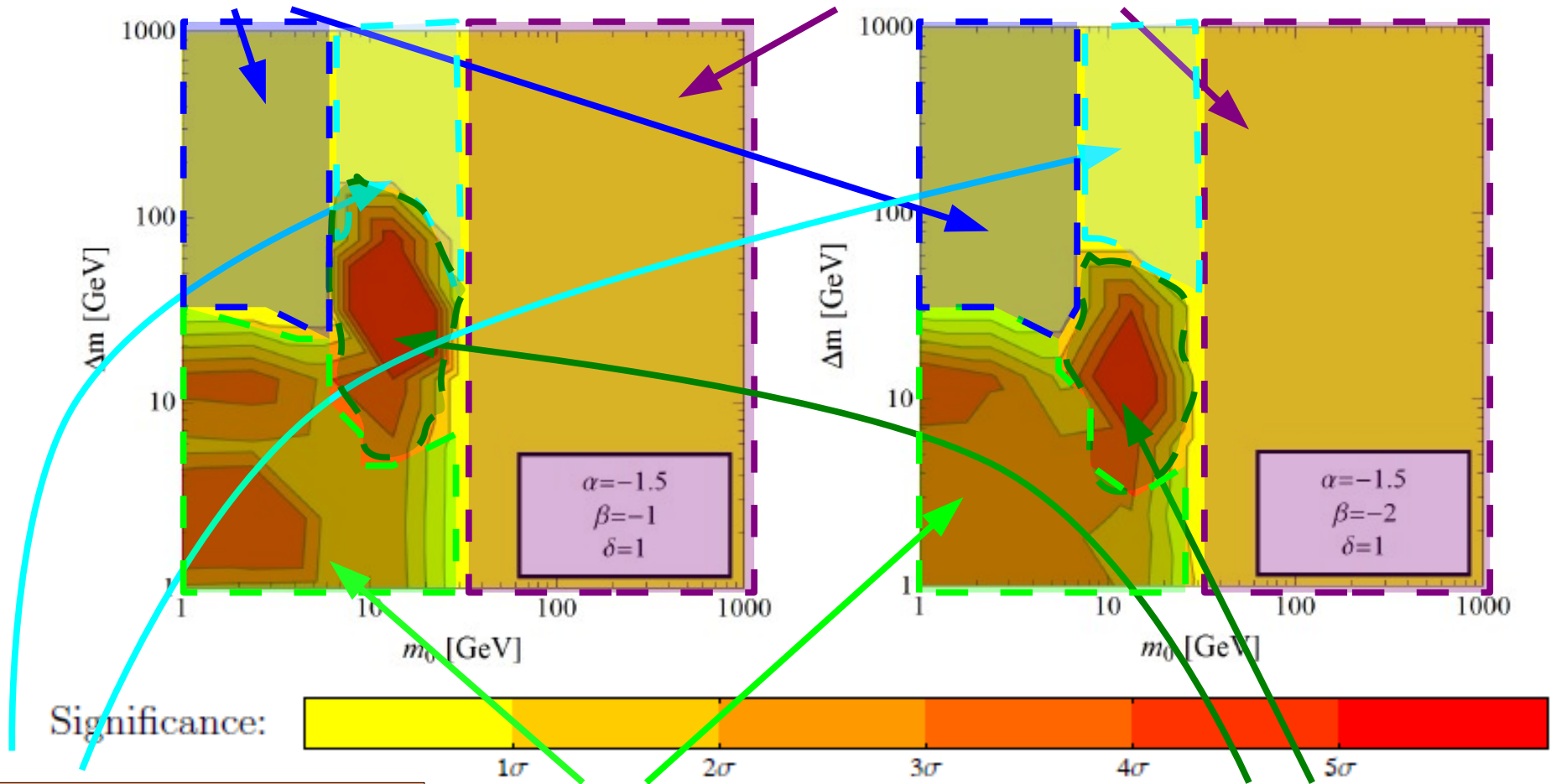
Next-to-lightest constituent χ_1 dominates the width of ψ .

$\text{BR}(\psi \rightarrow jj\chi_0) \approx \text{BR}(\psi \rightarrow jj\chi_1)$: two distinct m_{jj} peaks.

Distinguishing DDM Ensembles: Results

χ_0 contributes mostly at $E_R < E_R^{\min}$,
all other χ_j in high-mass regime

All χ_n in high-mass regime: little difference
between their dR/dE_R contributions



Only χ_0 contributes perceptible to overall rate: looks like regular low-mass DM

Multiple χ_j in low-mass region: distinctive dR/dE_R spectra

χ_0 in low-mass regime, all χ_j with $j \geq 1$ in high-mass regime: kink in dR/dE_R spectrum